ACS OMEGA

Open Access

http://pubs.acs.org/journal/acsodf

Article

One-Pot Sequential Synthesis of Alkenylated Dihydroquinolinones and Hexahydroacridinones in Deep Eutectic Solvent Medium

Sundararajan Suresh and Fazlur Rahman Nawaz Khan*

Cite This: *ACS Omega* 2024, 9, 36198−36219

Read Online

ACCESS | Metrics & More | Article Recommendations | Supporting Information

ABSTRACT: The sequential synthesis of *N*-heterocycles from saturated ketones poses significant challenges and has rarely been reported. Herein, an efficient synthesis of alkenylated dihydroquinolinones **7** and hexahydroacridinones **8** is achieved from saturated ketones **1** or **2** via dehydrogenation, cyclization, oxidation, and α-alkenylation in choline chloride-based deep eutectic solvent (DES) medium. This strategy provides alkenylated dihydroquinolinones **7** and hexahydroacridinones **8** in excellent yield from low-cost, readily available starting materials under environmentally benign conditions. Furthermore, the synthesized compounds (**4**, **5**, **7**, and **8**) were investigated for their photophysical properties through absorption and emission spectral studies.

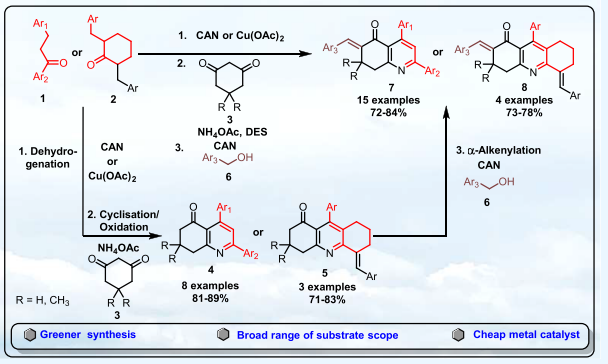

INTRODUCTION

Nitrogen heterocyclic scaffolds are prevalent in pharmaceutical lead compounds, natural products, and functional materials.[1−4] Specifically, dihydroquinolinone and hexahydroacridinone derivatives have attracted considerable interest due to their role as essential structural motifs and their presence in numerous natural products and drugs with diverse bioactivities,[5,6] including anticancer,[7−9] antipsychotic, HIV-1 RT-inhibiting,[10] anti-inflammatory,[11] hypertensive,[11] antibiotic,[12] and antidiabetic activity.[13] Some bioactive compounds containing dihydroquinolinone and hexahydroacridinone as the central core units are shown in Figure 1.[9,14−16]

Therefore, researchers have developed numerous synthetic strategies for the synthesis of these notable heterocycles. For example, in 2010, Srivastava and co-workers developed the stepwise synthesis of dihydroquinolinone derivatives via cyclization and dehydrogenation using chalcone, NH_4OAc, and 1,3-diketone (Scheme 1a, eq 1).[17] Later, in 2013, Mukhopadhyay and co-workers reported an MCM-41-supported hexafluorophosphoric acid-catalyzed synthesis of dihydroquinolinones through dehydrative cyclization followed by dehydrogenation utilizing aldehyde, acetophenone, 1,3-diketone, and $(NH_4)_2CO_3$.[18] In 2015, the same group investigated the Cu/SiO_2-catalyzed one-pot synthesis of dihydroquinolinones through condensation, Michael addition, and cyclization followed by oxidation using NH_4OAc as a nitrogen source (Scheme 1a, eq 2).[19] Recently, Yan and co-workers developed the iron-catalyzed synthesis of dihydroquinolinone derivatives using α,β-unsaturated ketoxime acetates and enaminones (Scheme 1a, eq 3).[20] Likewise, in 2014, Tkachev and co-workers reported the microwave-assisted, iron-catalyzed synthesis of hexahydroacridinone derivatives via condensation utilizing pinocarvone oxime and enamines (Scheme 1a, eq 4).[21] However, all the above-mentioned methods have faced several drawbacks, such as the usage of volatile organic solvents, unstable starting materials, and hazardous and expensive reagents.

Recently, researchers in academia and industry have aimed to develop the synthesis of pharmaceutically important molecules using green solvents to reduce chemical waste.[22−24] In this regard, deep eutectic solvents (DESs) are considered green solvents. DESs possess unique properties such as biodegradability, low toxicity, water solubility, recyclability, nonvolatility, low cost, and simple preparation.[25−30] Furthermore, DESs have potential applications in synthetic organic chemistry by serving as catalysts and solvents for organic transformations.[31−33]

Regarding this, our group has recently developed a DES-mediated synthesis of biologically active functionalized nitrogen heterocyclics including quinoline,[34−36] acridinone,[37] spirooxindoles,[38] benzophenanthroline, and benzonaphthyridine derivatives.[39] Continuing this line of research, we have now developed a choline chloride-based DES-mediated one-pot sequential synthesis of α-alkenylated dihydroquinolinones **7** and hexahydroacridinones **8** through dehydrogenation,

Received: March 5, 2024
Revised: July 8, 2024
Accepted: July 22, 2024
Published: August 16, 2024

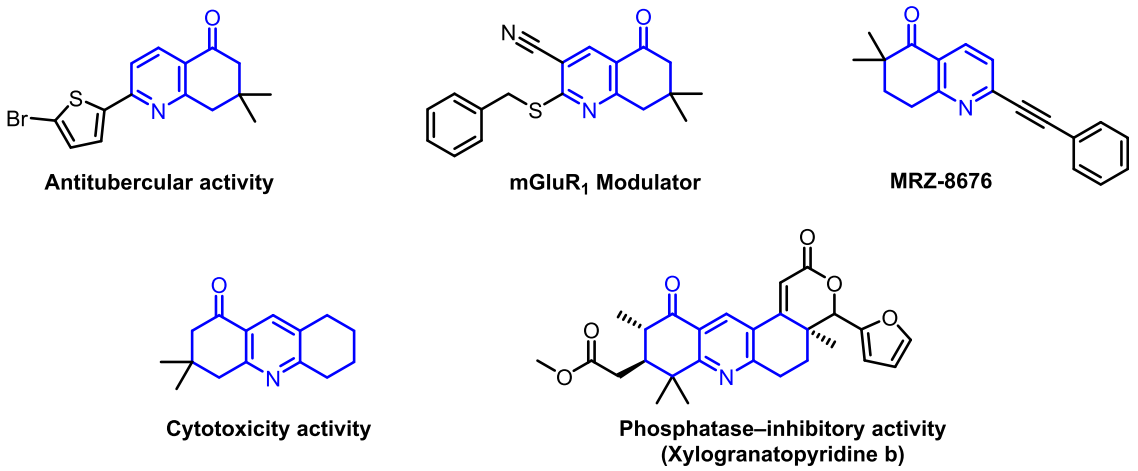

Figure 1. Bioactive compounds bearing dihydroquinolinone and hexahydroacridinone motifs.

cyclization, oxidation, and α-alkenylation from saturated ketones utilizing CAN or $Cu(OAc)_2$/TEMPO as a catalyst (Scheme 1b).

RESULTS AND DISCUSSION

To determine the optimized reaction conditions for the synthesis of dihydroquinolinone **4a** and hexahydroacridinone **5a** via dehydrogenation, cyclization followed by oxidation using saturated ketones **1a** or **2a**, diketones **3a**, and NH_4OAc under various reaction conditions has been investigated. A comprehensive optimization table for the synthesis of dihydroquinolinone **4a** and hexahydroacridinone **5a** is provided in the Supporting Information (Tables S1−S3).

Based on the optimization results (Tables S1−S3, Supporting Information), we determined that the optimal reaction conditions for synthesizing dihydroquinolinone **4a** involved saturated ketone **1a** (0.2 mmol), CAN (20 mol %) as an efficient catalyst, TEMPO (20 mol %) as an oxidant catalyst, and TBAB (100 mg) as reaction medium at 100 °C for 3 h to achieve the dehydrogenated ketone. Subsequently, diketone **3a** (0.2 mmol), NH_4OAc (2.0 mmol), and ChCl:PTSA (1:1) (200 mg) were added in O_2 atm, and the reaction was continued by heating at 100 °C for 4 h, resulting in 85% yield of the dihydroquinolinone **4a**.

Likewise, for the optimal synthesis of hexahydroacridinone **5a**, we employed ketone **2a** (0.2 mmol), $Cu(OAc)_2$ (20 mol %) as a catalyst, TEMPO (20 mol %) as an oxidant catalyst, 2,2′-bipyridyl (20 mol %) as a ligand, and TBAA (100 mg) as reaction medium at 100 °C for 3 h to achieve the formation of the unsaturated ketone. Then, we added diketone **3a** (0.2 mmol), NH_4OAc (2.0 mmol), and ChCl:PTSA (1:1) in O_2 atm and continued heating at 100 °C for 4 h, resulting in 83% yield of the desired product **5a**.

The optimizations, including the variation of catalysts, oxidants, ligands, N-source, temperatures, and solvents, were explored as explained in the Supporting Information (Tables S1−S3). The key findings are summarized in Table 1, as discussed below. Under the standard optimized conditions, dihydroquinolinone **4a** was obtained in 85% yield, while hexahydroacridinone **5a** was obtained in 83% yield (Table 1, entry 1). Decreasing the load of NH_4OAc, utilizing various DESs, and varying temperatures resulted in decreased yields of products **4a** or **5a** (Table 1, entries 2−5). In the absence of a catalyst or oxidant catalyst, the corresponding product **4a** or **5a** was not formed (Table 1, entries 6−7). When the reaction was carried out in the absence of TBAX (X = Br), the yield of **4a** was decreased, and in the absence of TBAX (X = OAc), product **5a** was not observed (Table 1, entry 8). In the reaction examined in the absence of a ligand, the dihydroquinolinone **4a** yield was 85%, whereas the hexahydroacridinone **5a** product was not observed (Table 1, entry 9), underscoring that the ligands play a crucial role in the synthesis of **5a**. Entries 2−9 demonstrate that a combination of CAN, TEMPO, TBAB, and ChCl:PTSA (1:1) is necessary for the formation of **4a**. Upon changing the ligands, the **5a** product formation was affected (Table 1, entry 10). Decreasing the load of the oxidant and catalyst has resulted in the detrimental yields of both **4a** and **5a** products (Table 1, entries 11, 12). Furthermore, a decrease in the load of ligands led to a decreased yield of product **5a** (Table 1, entry 13).

We further investigated the scope of substrates suitable for the synthesis of **4** and **5** by employing the optimized reaction conditions from Table 1, entry 1, and the results are tabulated in Table 2. Various unsymmetrical saturated ketones were efficiently transformed into the desired products through this method. The synthesis of dihydroquinolinones **4**, by employing a range of neutral (H) and electron-donating group (EDG) (CH_3 and OCH_3)-substituted unsymmetrical saturated ketones **1**, along with diketones (H), gave a good yield of **4a**−**4c** (83−85%). Conversely, when electron-withdrawing groups (EWGs) (Br or F) were present in the unsymmetrical saturated ketones **1**, reactions with substituted diketones (H or CH_3) resulted in higher yields of **4d**−**4e** (86−89%). The EWG-substituted unsymmetrical saturated ketones exhibited higher yields compared to the EDG-substituted saturated ketones. When the reaction was conducted using EDG-substituted unsymmetrical saturated ketones **1** with EDG-substituted diketones (CH_3), it resulted in the formation of the desired products (**4f**, **4g**) with yields ranging from 81 to 85%. Notably, the EDG substitution in diketones (CH_3) did not significantly affect the yield. Additionally, the reaction was explored with alkyl alkanoates, providing 82% yield of the desired product (**4h**).

Similarly, in the synthesis of hexahydroacridinones (**5a**, **5b**), employing electron-neutral (H) and EWG (Cl)-substituted symmetrical saturated ketones **2** yielded 81−83% of **5a** and **5b**. In particular, the EWG-substituted symmetrical saturated ketone **2** yielded less than those with neutral substituents.

https://doi.org/10.1021/acsomega.4c02058
ACS Omega 2024, 9, 36198−36219

Scheme 1. (a) Previous Work: (1) Synthesis of Dihydroquinolinones and (2) Synthesis of Hexahydroacridinones and (b) Present Work: Synthesis of Dihydroquinolinone and Hexahydroacridinone Derivatives

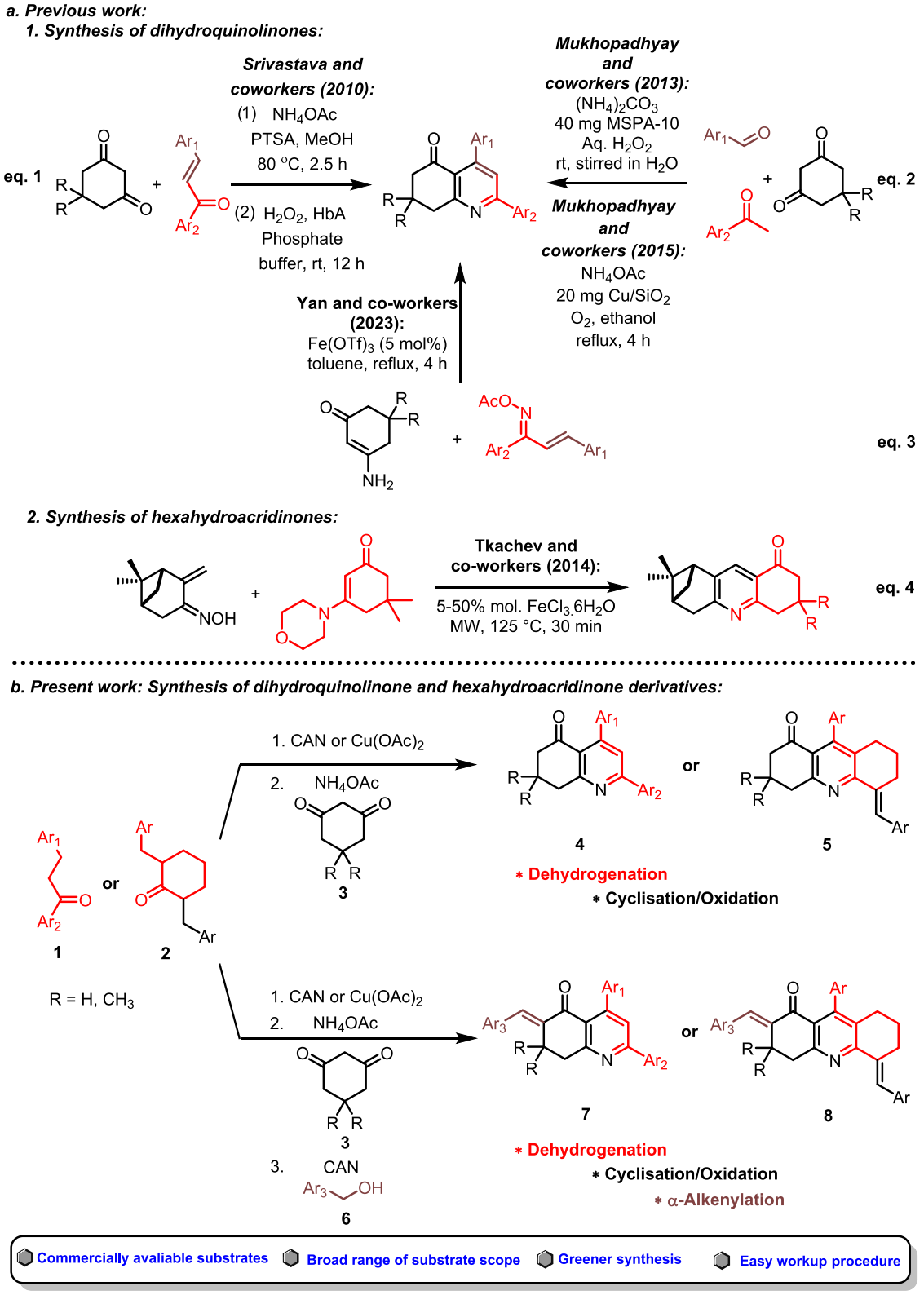

Moreover, when we investigated the reaction with heterocyclic symmetrical saturated ketone **2**, it resulted in 71% yield of **5c** (Table 2).

Moreover, we explored a one-pot sequential synthesis for α-alkenylated dihydroquinolinones **7a** and hexahydroacridinones **8a** by examining the various reaction conditions. The complete optimization, including variations in the metal catalyst, oxidant, solvent, and temperature, was conducted as outlined in the Supporting Information (Tables S4 and S5). The notable deviation from the optimized conditions is discussed below

https://doi.org/10.1021/acsomega.4c02058
ACS Omega 2024, 9, 36198−36219

Table 1. Optimization Study for the Synthesis of 4a and 5a[a,b]

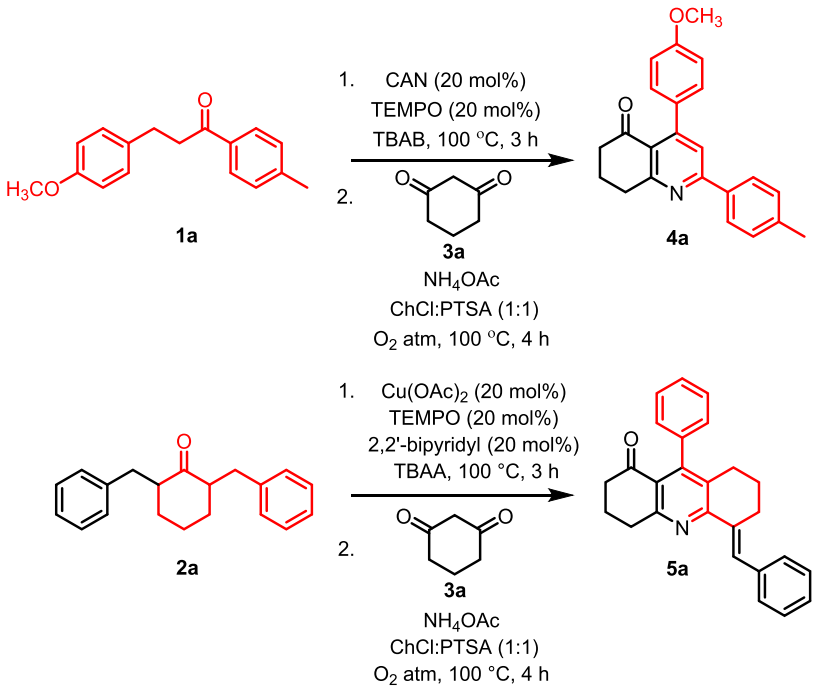

entry	variation from the optimized conditions	yield[c] (%) 4a	5a
1.	none[a,b]	85	83
2.	decrease NH_4OAc loading (2.0−8.0 equiv)	<71	<63
3.	other choline chloride-based DES	<65	<52
4.	decreased temperature (90 °C)	52	40
5.	increased temperature (110 °C)	80	76
6.	absence of the catalyst	-	-
7.	absence of the oxidant	-	-
8.	absence of TBAX (X = Br, OAc)	<10	-
9.	absence of the ligand	85	-
10.	other ligands	NA	<65
11.	decreasing oxidant loading (10 mol %)	54	39
12.	decreasing catalyst loading (10 mol %)	68	51
13.	decreasing ligand loading (10 mol %)	NA	42

[a]Standard reaction conditions for **4a**: **1a** (0.2 mmol), CAN (20 mol %), TEMPO (20 mol %), and TBAB (100 mg) were added at 100 °C for 3 h. Then, **3a** (0.20 mmol), NH_4OAc (2.0 mmol), and ChCl:PTSA (1:1 mmol) (200 mg) were added in O_2 atm at 100 °C for 4 h. [b]Standard reaction conditions for **5a**: **2a** (0.2 mmol), $Cu(OAc)_2$ (20 mol %), TEMPO (20 mol %), 2,2′-bipyridyl (20 mol %), and TBAA (100 mg) were added at 100 °C for 3 h. Then, **3a** (0.20 mmol), NH_4OAc (2.0 mmol), and ChCl:PTSA (1:1 mmol) (200 mg) were added in O_2 atm at 100 °C for 4 h. [c]Isolated yields.

(Table 3). The optimized reaction conditions (Tables S4 and S5, Supporting Information) for the synthesis of **7a** and **8a** involved several steps. Initially, the reaction was performed by following the standard reaction conditions from Table 1 to obtain **4a** or **5a**. Subsequently, the reaction proceeded by introducing alcohol **6a** or **6b**, CAN (10 mol %) as a catalyst, and TEMPO (10 mol %) as an oxidant in ChCl:PTSA (1:1) medium at 100 °C to achieve a generous yield (79%) of α-alkenylated dihydroquinolinone **7a** and α-alkenylated hexahydroacridinone **8a** (73%) (Table 3, entry 1).

When the reaction was performed under the standard reaction conditions from Table 1 and continued with the addition of an aldehyde instead of alcohol **6a** and an additional DES at 100 °C, it provided the α-alkenylated dihydroquinolinone **7a** in 70% yield. Likewise, the hexahydroacridinone **5a** reaction with an aldehyde instead of alcohol **6b** and an additional DES provides 63% of α-alkenylated hexahydroacridinone **8a** (Table 3, entry 2). The α-alkenylation of ketone with other catalysts ($RuCl_3$, $NiCl_2$) gave less than 35% yield of **7a** and less than 10% of **8a** (Table 3, entry 3). Further screening of the reaction with other choline chloride-based DES catalysts or solvents yielded less than 38% of **7a** and less than 30% of **8a** (Table 3, entry 4). Furthermore, decreasing or increasing the reaction temperature as well as decreasing the loadings of the catalyst or oxidant resulted in decreased product yields of **7a** and **8a** (Table 3, entries 5−8). However, without the catalyst and oxidant, both α-alkenylated dihydroquinolinone **7a** and hexahydroacridinone **8a** were not formed (Table 3, entries 9−10).

Nevertheless, we investigated the substrate scope for the one-pot sequential synthesis of α-alkenylated dihydroquinolinones **7** and hexahydroacridinones **8** using the optimized

https://doi.org/10.1021/acsomega.4c02058
ACS Omega 2024, 9, 36198−36219

Table 2. Substrate Scope for the Synthesis of Dihydroquinolinones 4 and Hexahydroacridinones 5[a]

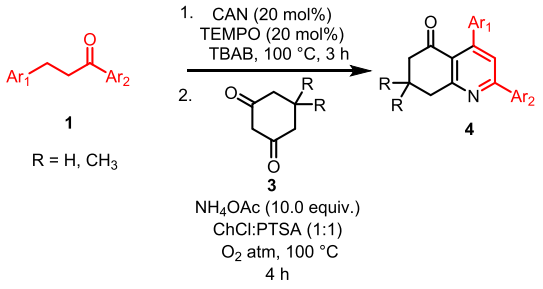

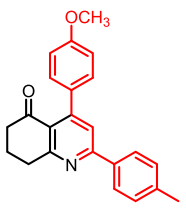
4a, 85%


4a
(CCDC: 2201957)

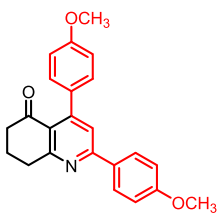
4b, 83%

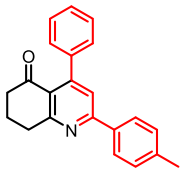
4c, 84%

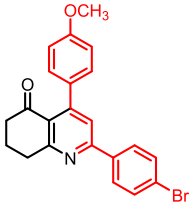
4d, 89%

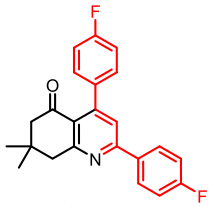
4e, 86%

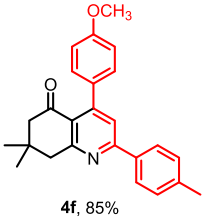
4f, 85%

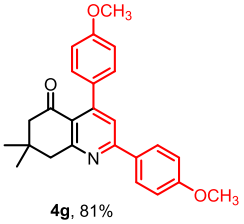
4g, 81%

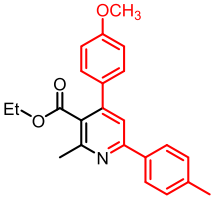
4h, 82%

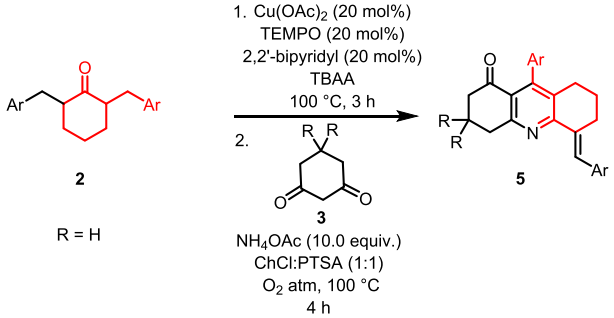

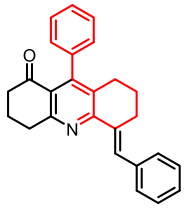
5a, 83%

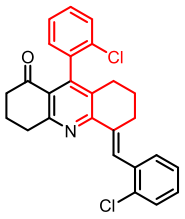
5b, 81%

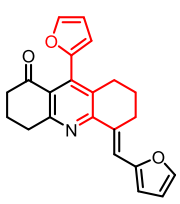
5c, 71%

[a]All reactions were performed according to the standard reaction conditions given in Table 1 (entry 1).

https://doi.org/10.1021/acsomega.4c02058
ACS Omega 2024, 9, 36198−36219

Table 3. Optimization Study for the One-Pot Synthesis of 7a[a] and 8a[b]

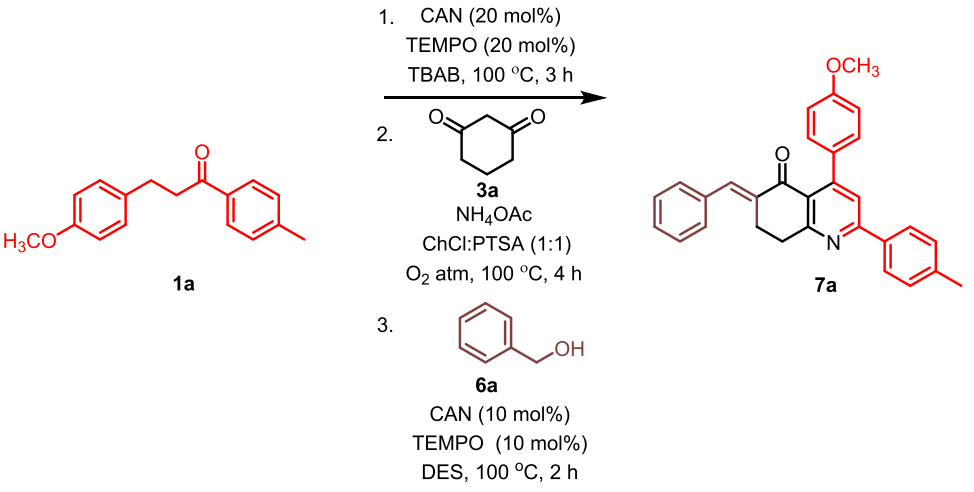

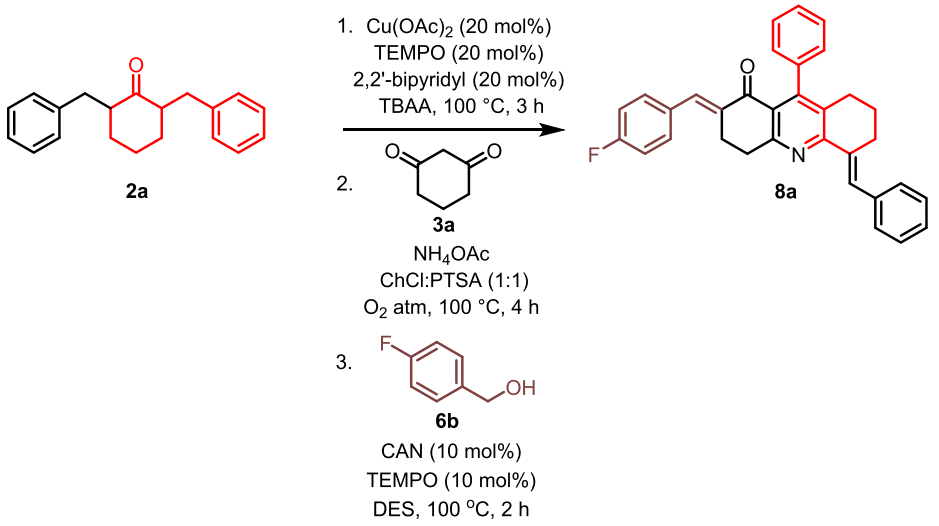

entry	variation from the optimized conditions	yield[c] (%) 7a	8a
1.	none[a,b]	79	73
2.	using aldehyde instead of alcohol	70	63
3.	other catalysts ($RuCl_3$, $NiCl_2$) used instead of CAN	<35	<10
4.	other choline chloride-based DESs	<38	<30
5.	decreased temperature (90 °C)	48	32
6.	increased temperature (100 °C)	76	68
7.	decreasing catalyst loading (5 mol %)	51	45
8.	decreasing oxidant loading (5 mol %)	44	34
9.	absence of CAN	-	-
10.	absence of TEMPO	-	-

[a]Standard reaction conditions for **7a**: **1a** (0.2 mmol), CAN (20 mol %), TEMPO (20 mol %), and TBAB (100 mg) were added at 100 °C for 3 h. Then, **3a** (0.20 mmol), NH_4OAc (2.0 mmol), and ChCl:PTSA (1:1 mmol) (200 mg) were added under O_2 atm at 100 °C and heated for 4 h, followed by the addition of **6a** (0.2 mmol), CAN (10 mol %), TEMPO (10 mol %), and ChCl:PTSA (1:1 mmol) (200 mg) at 100 °C and maintained for 2 h. [b]Standard reaction conditions for **8a**: **2a** (0.2 mmol), $Cu(OAc)_2$ (20 mol %), TEMPO (20 mol %), 2,2′-bipyridyl (20 mol %), and TBAA (100 mg) were added at 100 °C for 3 h. Then, **3a** (0.20 mmol), NH_4OAc (2.0 mmol), and ChCl:PTSA (1:1 mmol) (200 mg) were added in O_2 atm at 100 °C and heated for 4 h, followed by the addition of **6b** (0.2 mmol), CAN (10 mol %), TEMPO (10 mol %), and ChCl:PTSA (1:1 mmol) (200 mg) at 100 °C and maintained for 2 h. [c]Isolated yields.

conditions (Table 3, entry 1), and the results are summarized in Table 4. When α-alkenylated dihydroquinolinone synthesis was carried out with various neutral (H) group-, EDG (CH_3 and OCH_3)-, and EWG (Br)-substituted unsymmetrical saturated ketone **1** with electron-neutral (H) group-, EDG (CH_3, OCH_3, and $N(CH_3)_2$)-, and EWG (F and Cl)-substituted alcohols **6**, a moderate to good yield of **7a**−**7l** and **7n**−**7o** (72−84%) was achieved. The EDG-substituted alcohol provides a higher yield compared to the EWG-substituted alcohol. When the reaction was carried out with α,β-unsaturated alcohol, it resulted in 77% yield of the corresponding product (**7m**). Further synthesis of α-

https://doi.org/10.1021/acsomega.4c02058
ACS Omega 2024, 9, 36198−36219

Table 4. Scope of One-Pot Sequential Synthesis of α-Alkenylated Dihydroquinolinones 7[a,b] and Hexahydroacridinones 8[a,b]

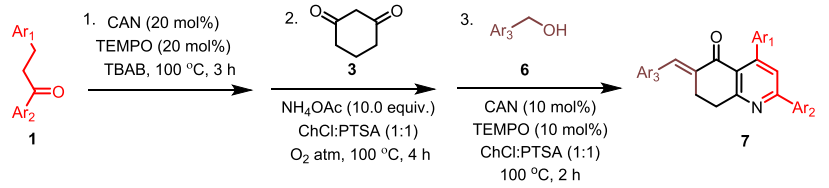

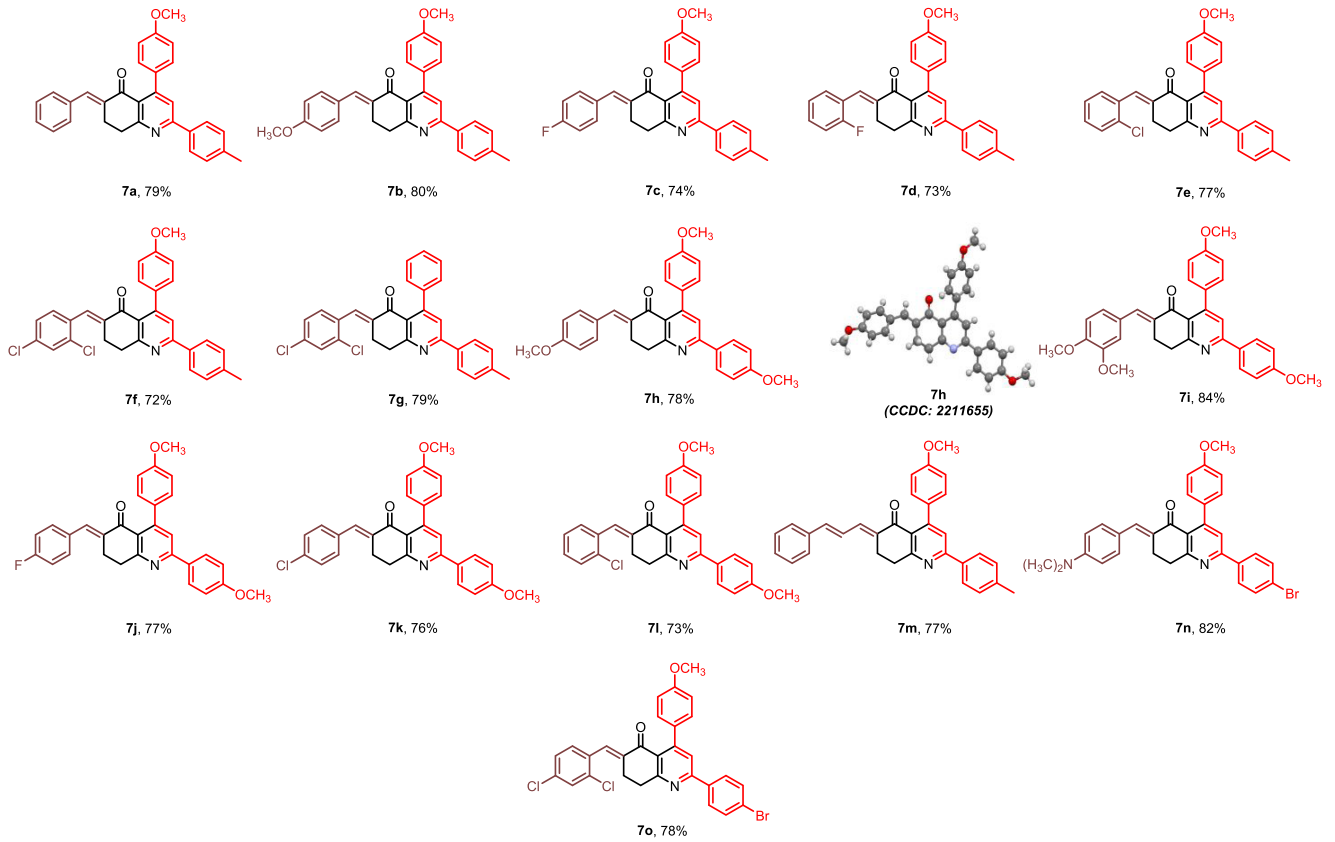

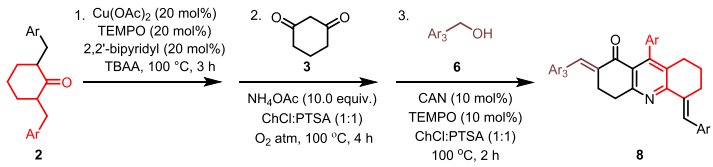

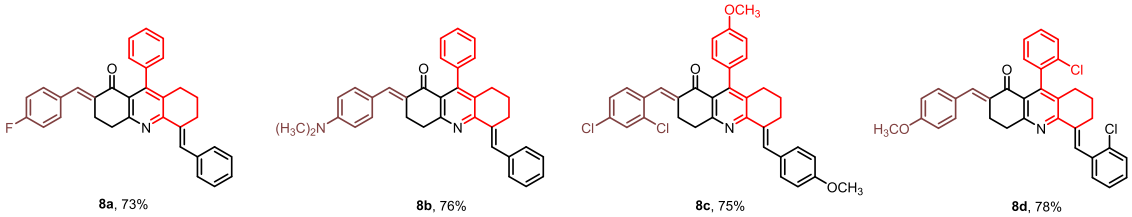

[a,b]All reactions were conducted according to the standard reaction conditions given in Table 3 (entry 1).

alkenylated hexahydroacridinone **8** was conducted using electron-neutral (H) group-, EDG (OCH_3)-, and EWG (Cl)-substituted symmetrical saturated ketone **2** with EDG (OCH_3 and $N(CH_3)_2$)- and EWG (F and Cl)-substituted alcohols, resulting in moderate to good yields of the desired products **8a**−**8d** (73−78%) (Table 4). Especially, when the reaction was performed with the EWG-substituted symmetrical saturated ketone **2** and EDG-substituted alcohol **6**, it provided a higher yield (**8d**) compared to other alkenylated hexahydroacridinone (**8a**−**8c**).

The structure of **4a** and **7h** was confirmed by single-crystal X-ray analysis (the ORTEP view is shown in Tables 2 and 4) (CCDC: 2201957, 2211655). Furthermore, **7l** was confirmed

https://doi.org/10.1021/acsomega.4c02058
ACS Omega 2024, 9, 36198−36219

Scheme 2. Proposed Mechanistic Pathways for the Synthesis of α-Alkenylated Dihydroquinolinone (7)

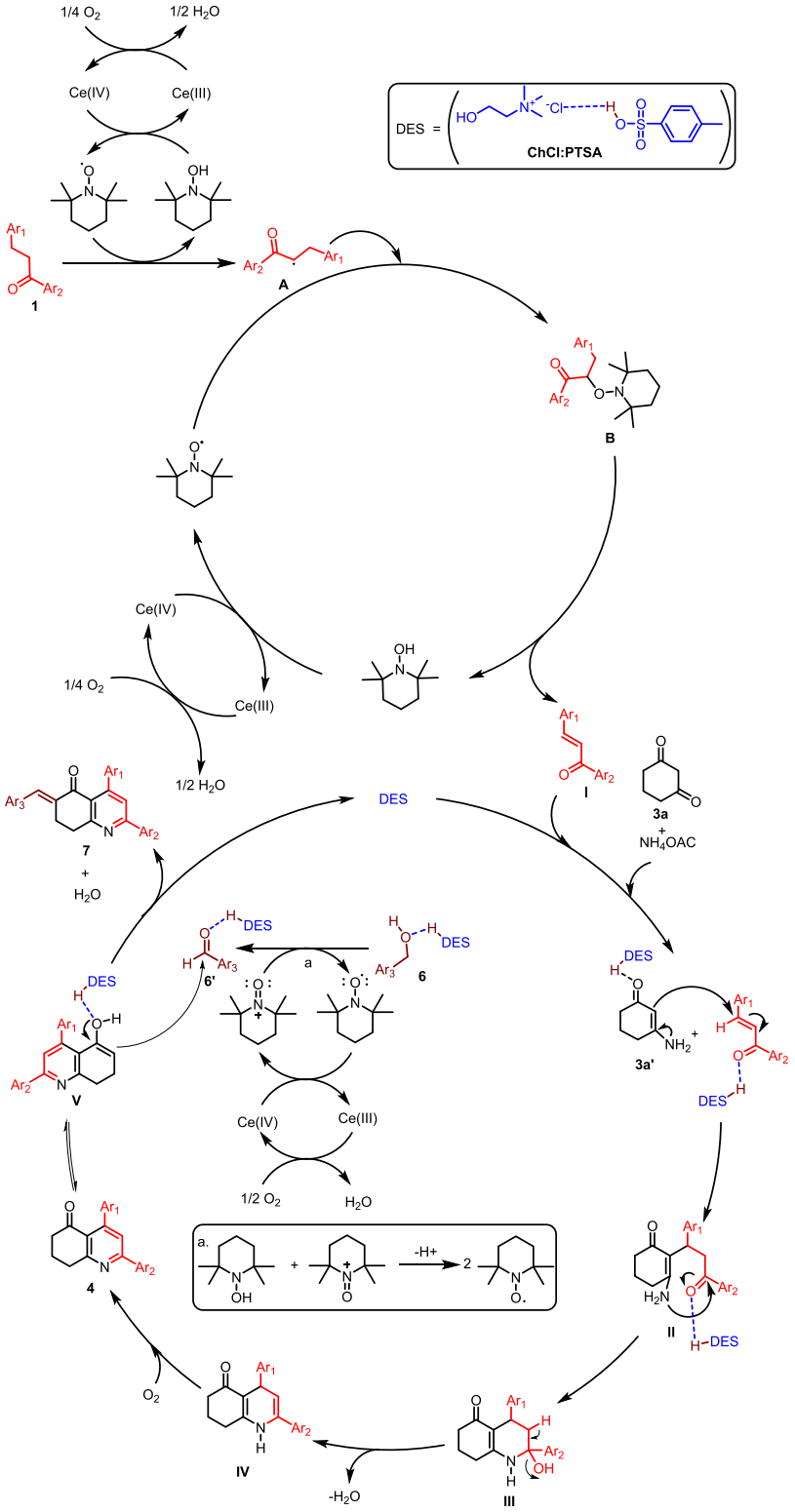

by two-dimensional (2D) spectroscopic studies, as explained in Supporting Information S16 and S17.

To understand the role of the catalyst, oxidant, solvent, and DES in the sequential synthesis of α-alkenylated dihydroquinolinone 7, a series of control experiments were conducted and are shown in the Supporting Information (Scheme S1). Reaction condition 1: In step 1, TBAB played a crucial role in converting saturated ketone **1a** to **1a′**. Similarly, in step 2, the ChCl:PTSA (1:1) DES is essential for the conversion of **1a′** to **4a**. Reaction condition 2: CAN as a catalyst and TEMPO as an oxidant were used for the oxidation of alcohol and DES was utilized for the formation of α-alkenylated products. This indicates that the DES acts as a solvent as well as a catalyst for the step 3 reaction. Reaction condition 3: Utilizing tetrahydro-

https://doi.org/10.1021/acsomega.4c02058
ACS Omega 2024, 9, 36198−36219

Scheme 3. Proposed Mechanistic Pathways for the Synthesis of α-Alkenylated Hexahydroacridinone (8)

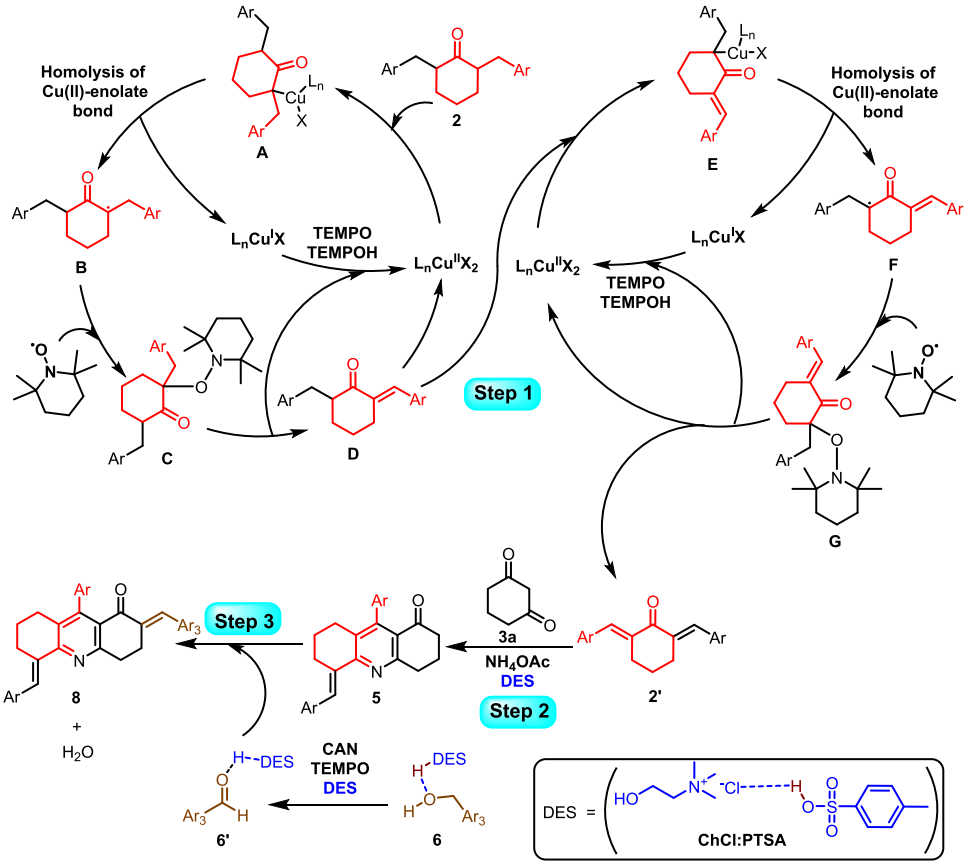

5*H*-chromen-5-one **13** instead of **4a** did not lead to the feasible formation of the α-alkenylated product **14**.

A plausible reaction mechanism for the synthesis of α-alkenylated dihydroquinolinone **7** is proposed based on our control experiments (Scheme S1, Supporting Information) and previously reported literature,[18,19,40−414243] which is illustrated in Scheme 2. Initially, TEMPO abstracts the hydrogen from saturated ketone **1**, forming radical intermediate **A** (this process involves the O_2 (dioxygen) being reduced to water (H_2O) through the oxidation of Ce^{3+} to Ce^{4+}, and at the same time, TEMPOH is oxidized to the TEMPO form through the conversion of Ce^{4+} to Ce^{3+}). Then, radical intermediate **A** reacts with TEMPO to form α-TEMPO-substituted ketone intermediate **B**. After that, intermediate **B** was converted into chalcone intermediate **I** and TEMPOH. Subsequently, molecular oxygen (O_2) is reduced to form H_2O through the oxidation of Ce^{3+} to Ce^{4+}. Meanwhile, TEMPOH is oxidized to TEMPO, which is achieved through the conversion of Ce^{4+} to Ce^{3+}, and this process completes the dehydrogenation of the saturated ketone cycle. In the second step, chalcone intermediate **I** reacts with diketone **3a** and NH_4OAc via a Michael-type addition reaction to form intermediate **II**. Next, intermediate **II** undergoes cyclization, followed by dehydration, leading to the formation of intermediate **IV**. Subsequently, intermediate **IV** readily undergoes dehydrogenation in an oxygen atmosphere to form the dihydroquinolinone intermediate **4**. Further, the dihydroquinolinone intermediate **4** undergoes enolization in DES medium, forming intermediate **V**.[18,19] Meanwhile, dioxygen (O_2) was reduced to H_2O through the oxidation of Ce^{3+} into Ce^{4+}, and TEMPO got oxidized to an *N*-oxoammonium cation with the aid of Ce^{4+} into Ce^{3+}. After that, the *N*-oxoammonium cation oxidizes alcohol **6** to form aldehyde **6′**.[42,43] Finally, intermediate V underwent a reaction with aldehyde **6′** and provided the α-alkenylated dihydroquinolinone product **7**.

Similarly, a series of control experiments were performed to elucidate the reaction mechanism for the synthesis of alkenylated hexahydroacridinone **8**, as shown in the Supporting Information (Scheme S2). Reaction condition 1: In step 1, TBAA played a crucial role in converting saturated ketone **2a** to **2a′**, and in the step 2 reaction condition, the ChCl:PTSA (1:1) DES is essential for the conversion of **2a′** to **5a**. Reaction condition 2: DES serves as a solvent and catalyst for the step 2 reaction.

A plausible reaction mechanism for the synthesis of **8** is proposed based on our control experiments (Scheme S2, Supporting Information) and previously reported literature,[18,19,42−434445] which is presented as Scheme 3. Initially, Cu(II) reacts with saturated ketone **2** to form the metal-enolate complex **A**. After that, homolysis of the Cu(II)-enolate bond generates the intermediate **B**. Then, the intermediate **B** readily reacts with TEMPO to form the α-TEMPO-substituted ketone **C**. Further, the α-TEMPO-substituted ketone **C** undergoes the fast elimination of TEMPOH, resulting in the formation of intermediate **D**. After that, the intermediate **D** reacts with Cu(II) to form the metal-enolate complex **E**. Then, the intermediate **F** is formed by the homolysis of the Cu(II)-enolate bond. Further, the intermediate **F** reacts with TEMPO to form the α-TEMPO-substituted intermediate **G**. Then, it undergoes the fast elimination of TEMPOH to form the chalcone intermediate **2′**.[44−47] The step 2 and step 3 mechanisms follow similar mechanisms as in Scheme 2.

https://doi.org/10.1021/acsomega.4c02058
ACS Omega 2024, 9, 36198−36219

Scheme 4. (a) Scale-Up Batch and (b) Synthetic Application

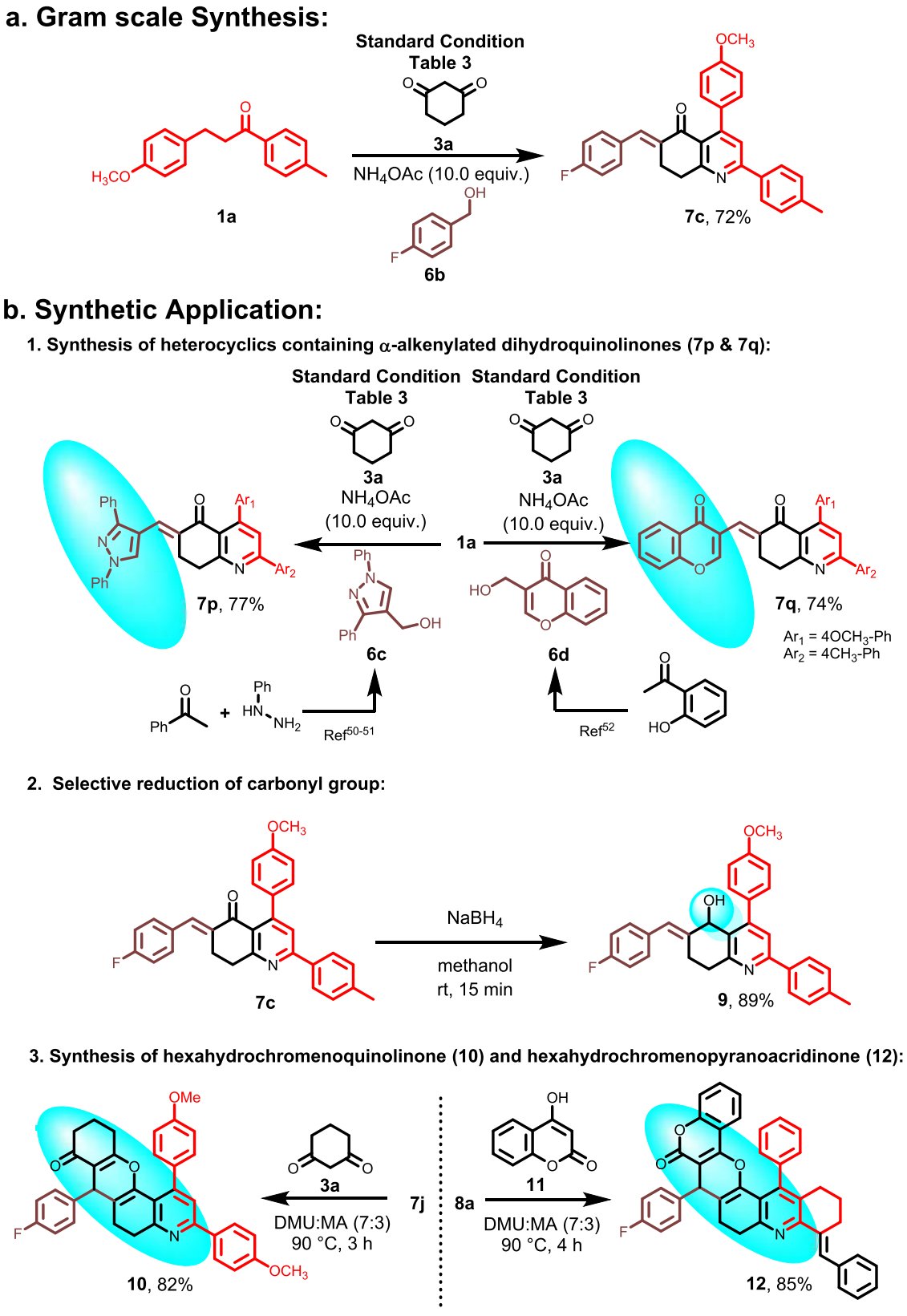

Generally, most of the fluoro-substituted alkenylated quinolinone motifs are more biologically potent molecules.[48,49] Therefore, we explored the gram-scale applicability of the current approach for the synthesis of alkenylated dihydroquinolinones (**7c**). The reaction was scaled up to 1.27 g of saturated ketone **1a** and conducted under the standard conditions from Table 3, utilizing diketone **3a**, NH_4OAc, and alcohol **6b**, yielding 72% of the desired product **7c** (Scheme 4a).

https://doi.org/10.1021/acsomega.4c02058
ACS Omega 2024, 9, 36198−36219

Furthermore, we investigated the synthetic utility of the synthesized alkenylated dihydroquinolinone **7** and hexahydroacridinone **8** compounds (Scheme 4b).

1. Synthesis of α-alkenylated dihydroquinolinones **7p** and **7q**: Alcohol **6c** or **6d** was used under the standard reaction conditions from Table 3 to yield 77% of the pyrazole-containing product **7p** and 74% of the chromone-containing product **7q**.
2. Selective reduction of the carbonyl group: The carbonyl group in compound **7c** was selectively reduced using $NaBH_4$ as a reducing agent in a methanol solvent at room temperature for 15 min, resulting in an 89% yield of the expected product (**9**).
3. Synthesis of hexahydrochromenoquinolinone **10** and hexahydrochromenopyranoacridinone **12**: The hexahydrochromenoquinolinone **10** was synthesized via Michael addition followed by intramolecular cyclization using compound **7j** and diketone **3a** in DMU:malonic acid DES medium at 90 °C for 3 h to afford 82% yield; similarly, the hexahydrochromenopyranoacridinone **12** was synthesized via Michael addition followed by intramolecular cyclization of **8a** with **11** in DMU:malonic acid DES medium at 90 °C for 4 h to yield 85% of the corresponding product (**12**).

Photophysical Property. The photophysical properties of quinolinone (**4** and **7**) and acridinone (**5** and **8**) derivatives were investigated using UV−visible and fluorescence spectroscopy (Tables 5 and 6). This comprehensive study delved into the absorption, emission, solvatochromism, aggregation-induced emission (AIE), and acidochromism properties of the synthesized derivatives. The quinolinone (**4** and **7**) and acridinone (**5** and **8**) derivatives exhibited absorption bands in the visible region due to $\pi-\pi^*$ and $n-\pi^*$ electronic transitions of an intramolecular charge transfer nature. The **4**, **5**, **7**, and **8** series of compounds showed absorption ($c = 1.0 \times 10^{-5}$ M) and emission ($c = 1.0 \times 10^{-5}$ M) bands between 273.5 and 424 nm and 350 and 579 nm, respectively, in an acetonitrile solvent. The corresponding Stokes shifts ranged from 59.5 to 174.5 nm, as tabulated in Tables 5 and 6. From the absorption and emission spectral data, it is evident that compound **8b** has the highest emission band maximum of 579 nm and **4h** has the highest Stokes shift of 174.5 nm due to intramolecular charge transfer and the EDG ($-OCH_3$) present in the motif. Compound **7e** has observed the highest quantum yield of 0.94% in the acetonitrile solvent. The absorption and emission spectra of the **4**, **5**, **7**, and **8** series of compounds are shown in the Supporting Information (Figures S8−S11).

Table 5. Optical Spectroscopy Data for 4a−4h and 5a−5c Derivatives[a]

compd	λ_{abs} (nm)	λ_{em} (nm)	Φ_F (%)	Stokes shift (nm)
4a	295.5	371	0.11	75.5
4b	305	391	0.02	86
4c	292	356	0.07	64
4d	294	445	0.03	151
4e	287.5	350	0.11	62.5
4f	295.5	355	0.09	59.5
4g	305	395	0.10	90
4h	273.5	448	0.62	174.5
5a	348	437	0.10	89
5b	341	416	0.15	75
5c	338	498	0.14	160

[a]All the absorption ($c = 1.0 \times 10^{-5}$ M) and emission ($c = 1.0 \times 10^{-5}$ M) spectra were recorded in ACN solutions at room temperature. Fluorescence quantum yield was determined relative to quinine sulfate in 0.1 M H_2SO_4 ($\Phi_F = 0.54$) as a standard.

Table 6. Optical Spectroscopy Data for 7a−7q and 8a−8d Derivatives[a]

compd	λ_{abs} (nm)	λ_{em} (nm)	Φ_F (%)	Stokes shift (nm)
7a	338	446	<0.01	108
7b	350	440	0.07	90
7c	341	446	0.08	105
7d	336	446	0.05	110
7e	336	443	0.94	107
7f	337	447	0.12	110
7g	338	436	0.12	98
7h	360	448	0.13	88
7i	357	454	0.17	97
7j	348	436	0.06	88
7k	349	427	0.07	78
7l	350	442	0.05	92
7m	364	451	0.05	87
7n	424	574	0.07	150
7o	336	438	0.15	102
7p	355	448	0.16	93
7q	334	449	0.56	115
8a	368	441	0.03	73
8b	420	579	0.11	159
8c	373	493	0.44	120
8d	364	467	0.05	103

[a]All the absorption ($c = 1.0 \times 10^{-5}$ M) and emission ($c = 1.0 \times 10^{-5}$ M) spectra were recorded in ACN solutions at room temperature. Fluorescence quantum yield was determined relative to quinine sulfate in 0.1 M H_2SO_4 ($\Phi_F = 0.54$) as a standard.

In addition, to perform an aggregation-induced emission (AIE) study of **7n** in a water/DMSO mixture, we excited **7n** at 438 nm and observed the corresponding emission at 566 nm, as shown in Figure 2a. In the emission spectra, we observed that until 40% of the water/DMSO mixture, no significant difference was noted in the emission intensity. However, with further increases in the water percentage in the mixture of water/DMSO, the emission intensity has slowly increased. The maximum emission intensity was observed with a 60% water/DMSO mixture. This indicated the formation of the nanoparticles, as noted due to the Tyndall phenomenon and Mie light scattering. A further increase in the water percentage in the water/DMSO mixture decreased the emission intensity by 70−99% due to the aggregation-caused quenching (ACQ) effect. This phenomenon was observed due to the twisted intramolecular charge transfer (TICT) process of **7n**, resulting in the formation of the aggregation-caused quenching (ACQ) effect. This result revealed that compound **7n** reached its maximum intensity in a 60% water/DMSO mixture. Furthermore, it is visually confirmed in Figure 2b,2c.

Similarly, for the AIE study of **8b** in a water/DMSO mixture, it was excited at 433 nm, and emission was observed at 565 nm, as shown in the Supporting Information (Figure S15). In the emission spectrum, it was observed that up to 30% of the water/DMSO mixture resulted in a decrease in emission intensity. The maximum emission intensity was observed with a 60% water/DMSO mixture, indicating the formation of nanoparticles, as evidenced by the Tyndall phenomenon and

https://doi.org/10.1021/acsomega.4c02058
ACS Omega 2024, 9, 36198−36219

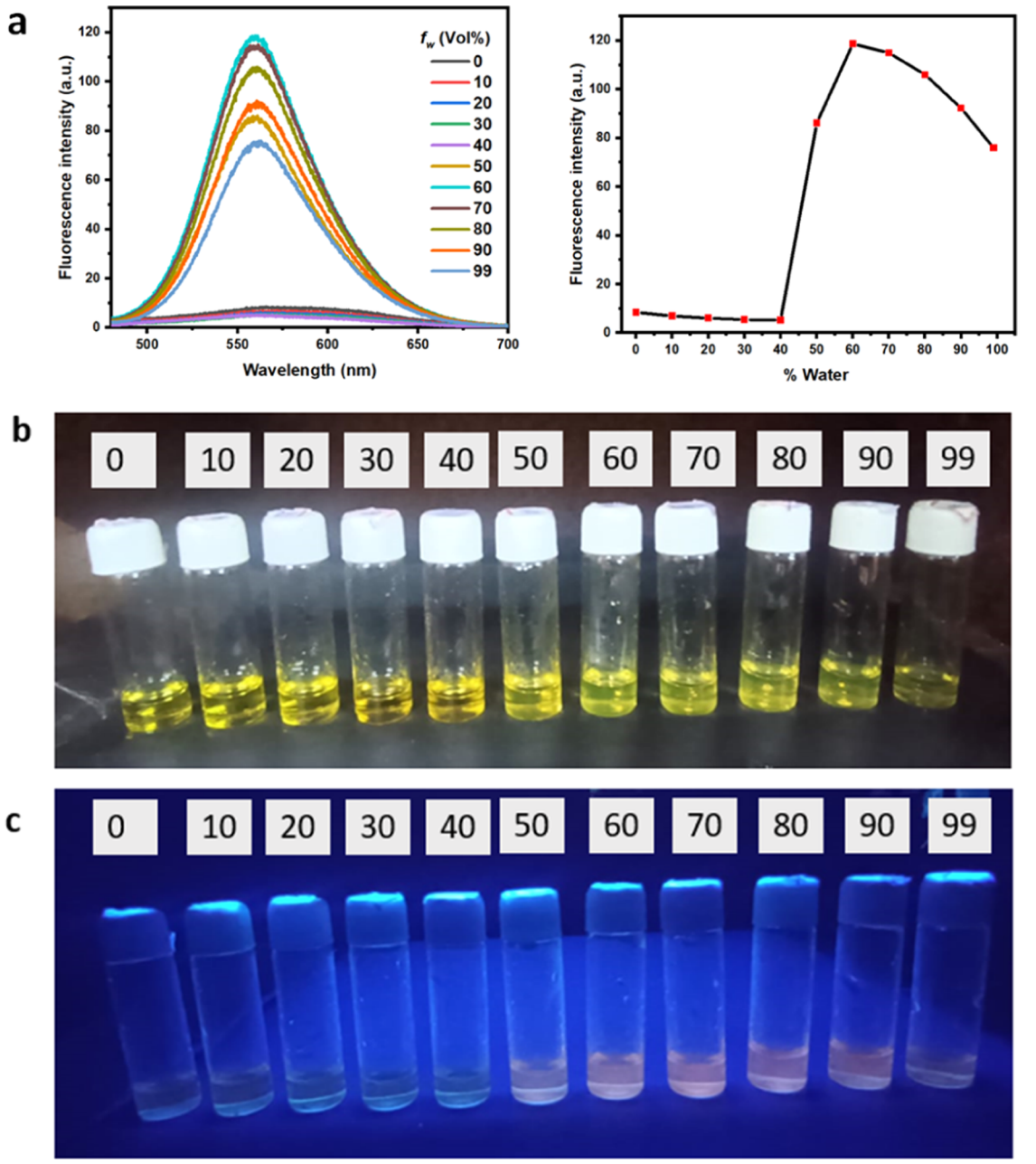

Figure 2. (a) Emission spectra of compound **7n** (50 μM) in a water/DMSO mixture with f_w = 0−99%, excited at 438 nm with the increasing percentage of the water fraction in the solution. (b) Photo image of **7n** in different water/DMSO mixtures under normal light. (c) Photo image of **7n** in different water/DMSO mixtures under 365 nm.

Scheme 5. Acidochromism Properties of 7n

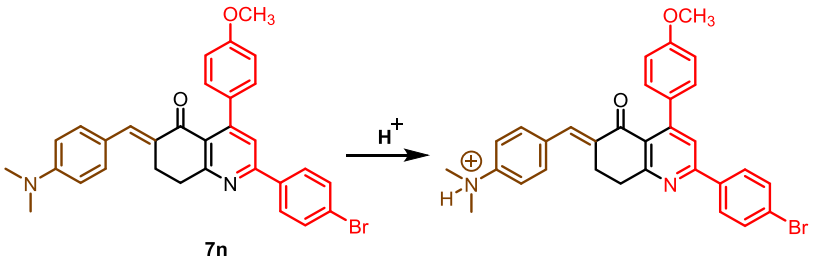

7n

Mie light scattering. However, with an increase in the percentage of water in the water/DMSO mixture, the emission intensity decreased slowly to 70−99%. This result reveals that compound **8b** achieved its maximum intensity in a 60% water/DMSO mixture.

https://doi.org/10.1021/acsomega.4c02058
ACS Omega 2024, 9, 36198−36219

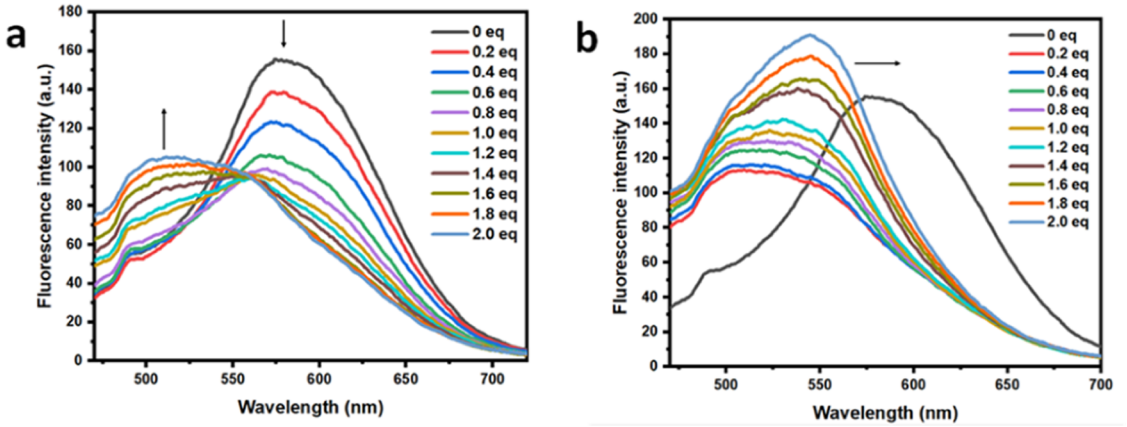

Figure 3. (a) Emission spectra of **7n** upon equivalent addition of TFA in ACN at 25 °C. (b) Emission spectra of **7n** upon equivalent addition of TEA in ACN at 25 °C.

Additionally, the acidochromism property of compound **7n** was investigated using trifluoroacetic acid (TFA) in an ACN solvent at room temperature (Scheme 5), and its emission spectra are shown in Figure 3. The emission spectral result revealed that upon the equivalent addition of trifluoroacetic acid (TFA) to **7n**, a blue shift is observed, accompanied by a gradual decrease in emission at 574 nm, and additionally, a new band was formed at 518 nm. This property indicates the formation of quaternary salts of **7n** (due to the *N*,*N*-dimethyl amino group of **7n** and the presence of TFA), leading to the deactivation of the resonance system. Conversely, with a proportional increase in the equivalent addition of triethyl amine (TEA), the emission exhibited a red shift.

Similarly, the acidochromism study for **8b** with TFA in an ACN solvent is presented in the Supporting Information (Figure S16). The emission spectral result reveals that the equivalent addition of TFA in **8b** to the formation of new peaks at 539 nm at the same time decreases the emission intensity at 581 nm. With the reversal addition of TEA in **8b**, the emission shifts to a red shift (555 nm).

Notwithstanding, the solvatochromism of different compounds, such as **4h**, **7h**, **7o**, and **8c**, was recorded in various polarities of organic volatile solvents, and the results are tabulated in Table 7. In the solvatochromism study, compound **8c** exhibited its highest emission at 508 nm in the DMSO solvent, while compound **7h** displayed the highest quantum yield of 45.63% in the pet ether solvent. Among the four derivatives, compound **4h** shows the highest Stokes shift of 167 nm in the DMSO solvent due to its solvent polarity and the electron-donating ($-OCH_3$) substituent in nicotinate motifs. Detailed optical studies revealed that all of the dihydroquinolinone and hexahydroacridinone derivatives showed a positive solvatochromism due to an increased emission with increasing solvent polarity. The absorption and emission spectra of compound **8c** in various polarities of organic solvents are shown in Figure 4. The absorption and emission spectra of compounds **4h**, **7h**, and **7o** were recorded in various polarities of organic solvents and are shown in the Supporting Information (Figures S12−S14).

The photophysical properties revealed that all the synthesized derivatives exhibit absorption and emission properties. Notably, compounds **7n** and **8b** exhibited the AIE and acidochromism properties. The AIE properties of compounds **7n** and **8b** will pave the way for potential applications in the development of OLED and chemosensor fields. Moreover, the acidochromism properties of **7n** and **8b** compounds have potential applications for the development of pH sensors.

Table 7. Solvatochromism Properties for 4h, 7h, 7o, and 8c[a]

compd	solvent	λ_{abs} (nm)	λ_{em} (nm)	Φ_F (%)	Stokes shift (nm)
4h	pet ether	262	363	2.55	101
	DCM	264	402	8.80	138
	EA	263	401	7.13	138
	DMSO	268	435	15.37	167
	MeOH	263	428	8.04	165
7h	pet ether	343	414	45.63	71
	DCM	363	435	0.29	72
	EA	354	444	0.13	90
	DMSO	364	439	0.27	75
	MeOH	355	440	16.20	85
7o	pet ether	330	393	0.04	63
	DCM	336	413	0.10	77
	EA	332	394	0.51	62
	DMSO	341	438	0.08	97
	MeOH	333	438	0.79	105
8c	pet ether	378	430	8.10	52
	DCM	390	470	0.05	80
	EA	381	445	3.00	64
	DMSO	389	508	0.21	119
	MeOH	384	501	4.57	117

[a]All the absorption ($c = 1.0 \times 10^{-5}$ M) and emission ($c = 1.0 \times 10^{-5}$ M) spectra were recorded in various polarities of solvents at room temperature. Fluorescence quantum yield was determined relative to quinine sulfate in 0.1 M H_2SO_4 ($\Phi_F = 0.54$) as a standard.

CONCLUSIONS

In summary, we synthesized α-alkenylated dihydroquinolinones and hexahydroacridinones from saturated ketones using a CAN- or $Cu(OAc)_2$/TEMPO-catalyzed dehydrogenation pathway in DES medium. The features of this reaction include the use of readily available starting materials, avoidance of volatile organic solvents, mild reaction conditions, and easy scalability for the production of α-alkenylated dihydroquinolinone compounds. Additionally, we explored the synthetic versatility of the synthesized compounds through selective reduction and Michael addition, followed by intramolecular cyclization. Optical studies revealed that derivatives **7n** and **8b** exhibit aggregation-induced emission (AIE) and acidochrom-

https://doi.org/10.1021/acsomega.4c02058
ACS Omega 2024, 9, 36198−36219

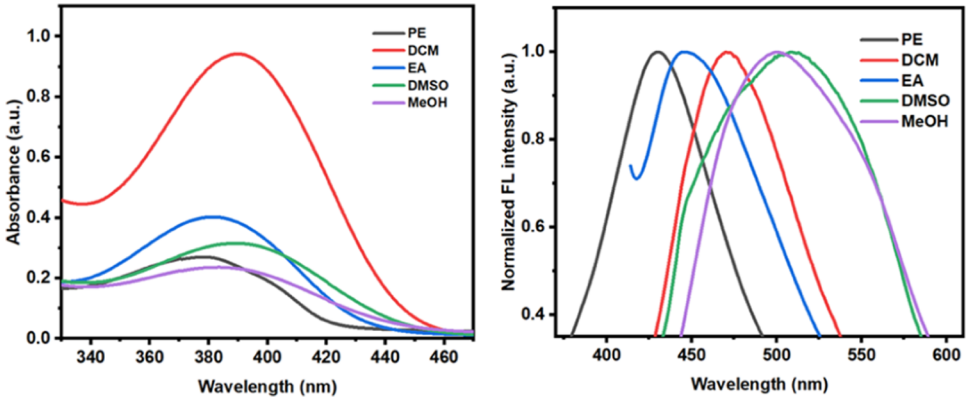

Figure 4. Absorption and normalized emission spectra of compound **8c** in various polarities of the solvent.

ism properties. Furthermore, the synthesized dihydroquinolinone, α-alkenylated dihydroquinolinone, and hexahydroacridinone derivatives exhibit positive solvatochromism. Moreover, the biological activities of the synthesized molecules are currently being investigated in our laboratory.

EXPERIMENTAL SECTION

General Information. All reactions were performed in oven-dried reaction tubes in a parallel synthesizer. Solvents and reagents were transferred at room temperature using oven-dried syringes and spatulas. The entire reaction was performed using glass reaction vials in a parallel synthesizer from App-Tec Instrument Ltd. The reagents and chemicals were purchased from Sigma-Aldrich, Merck, and TCI chemicals and were used without any purification. The reaction progress was monitored by Merck precoated alumina TLC sheets (F-254) using UV as a visualizing agent. Columns were packed as a slurry of silica gel in pet ether and ethyl acetate solvents. The reaction mixture was quenched in water and extracted with CH_2Cl_2 and the solvent was distilled out to provide crude products. Further crude products were purified by column chromatography on silica gel (100−200 meshes) from Merck Ltd. The ^1H and ^{13}C spectra were recorded in $CDCl_3$ or DMSO-d_6 using a Bruker AVANCE-III (400 MHz). Chemical shifts were reported in δ values (ppm) relative to $CDCl_3$ (^{1}**H NMR**: 7.26 ppm, ^{13}**C NMR**: 77.16 ppm) or TMS (0.00 ppm). The IR spectra were recorded on a Thermo Nicolet iS50 with an inbuilt ATR (Shimadzu IR Tracer-100) spectrometer. ν_{max} is reported in cm^{-1}. The X-ray single-crystal determination was performed on a D8-QUEST single-crystal XRD diffractometer. High-resolution mass spectra (HRMS) were recorded on a WATERS-XEVO G2-XS-QToF. The UV−visible absorption spectra were measured by a JASCO (V-670 PC). FL spectra were measured by a HITACHI (F-7000) fluorescence spectrophotometer.

General Procedure for the Synthesis of Dihydroquinolinone (4). To a saturated ketone **1** (0.2 mmol, 1.0 equiv), CAN (20 mol %) as a catalyst, TEMPO (20 mol %) as an oxidant, and TBAB (100 mg) were added in an oven-dried reaction vessel, and the mixture was allowed to stir at 100 °C for 3 h in the parallel synthesizer. After the complete formation of the dehydrogenative products, as monitored by TLC, 1,3-cyclohexadione **3** (0.2 mmol, 1.0 equiv), NH_4OAc (2.0 mmol, 10.0 equiv), and choline chloride:PTSA (1:1 mmol) (200 mg) were further sequentially added under O_2 atm at 100 °C and maintained for 4 h. After the complete formation of cyclized product **4** (as monitored by TLC), the reaction mixture was then diluted with water (20 mL) and the CH_2Cl_2 solvent, and the crude reaction mixture was extracted with CH_2Cl_2 (2 × 10 mL^2). The organic extracts were dried over anhydrous Na_2SO_4, and after the removal of CH_2Cl_2, the crude mixture was passed through silica-packed column chromatography to obtain the pure products **4a**−**4h** (81−89% yield).

General Procedure for the Synthesis of Hexahydroacridinone (5). To a saturated ketone **2** (0.2 mmol, 1.0 equiv), $Cu(OAc)_2$ (20 mol %) as a catalyst, TEMPO (20 mol %) as an oxidant, 2,2′-bipyridyl (20 mol %) as a ligand, and TBAA (100 mg) were added in an oven-dried reaction vessel, and the mixture was allowed to stir at 100 °C for 3 h in the parallel synthesizer. After the complete formation of dehydrogenative products, as monitored by TLC, 1,3-cyclohexadione **3** (0.2 mmol, 1.0 equiv), NH_4OAc (2.0 mmol, 10.0 equiv), and choline chloride:PTSA (1:1 mmol) (200 mg) were further sequentially added under O_2 atm at 100 °C and maintained for 4 h. After the complete formation of cyclized product **5** (as monitored by TLC), the reaction mixture was then diluted with water (20 mL) and the CH_2Cl_2 solvent, and the crude reaction mixture was extracted with CH_2Cl_2 (2 × 10 mL^2). The organic extracts were dried over anhydrous Na_2SO_4, and after the removal of CH_2Cl_2, the crude mixture was passed through silica-packed column chromatography to obtain the pure products **5a**−**5c** (71−83% yield).

General Procedure for the Synthesis of α-Alkenylated Dihydroquinolinone (7). To a saturated ketone **1** (0.2 mmol, 1.0 equiv), CAN (20 mol %) as a catalyst, TEMPO (20 mol %) as an oxidant, and TBAB (100 mg) were added in an oven-dried reaction vessel, and the mixture was allowed to stir at 100 °C for 3 h in the parallel synthesizer. After the complete formation of the dehydrogenative products, as monitored by TLC, 1,3-cyclohexadione **3** (0.2 mmol, 1.0 equiv), NH_4OAc (2.0 mmol, 10.0 equiv), and choline chloride:PTSA (1:1 mmol) (200 mg) were further sequentially added under O_2 atm at 100 °C and maintained for 4 h. After the complete formation of cyclized product **4**, substituted benzyl alcohol **6** (0.2 mmol, 1.0 equiv), CAN (10 mol %) as a catalyst, TEMPO (10 mol %) as an oxidant, and choline chloride:PTSA (1:1 mmol) (200 mg) were added at 100 °C and maintained for 2 h. After the complete formation of alkenylated product **7** (as monitored by TLC), the reaction mixture was then diluted with water (20 mL) and the CH_2Cl_2 solvent, and the crude reaction mixture was extracted with CH_2Cl_2 (2 × 10 mL^2). The organic extracts were dried over anhydrous Na_2SO_4, and after the removal of CH_2Cl_2, the crude mixture was passed

https://doi.org/10.1021/acsomega.4c02058
ACS Omega 2024, 9, 36198−36219

through silica-packed column chromatography to obtain the pure products **7a**−**7o** (72−84% yield).

General Procedure for the Synthesis of α-Alkenylated Hexahydroacridinone (8). To a saturated ketone **2** (0.2 mmol, 1.0 equiv), $Cu(OAc)_2$ (20 mol %) as a catalyst, TEMPO (20 mol %) as an oxidant, 2,2′-bipyridyl (20 mol %) as a ligand, and TBAA (100 mg) were added in an oven-dried reaction vessel, and the mixture was allowed to stir at 100 °C for 3 h in the parallel synthesizer. After the complete formation of the dehydrogenative products, as monitored by TLC, 1,3-cyclohexadione **3** (0.20 mmol, 1.0 equiv), NH_4OAc (2.0 mmol, 10.0 equiv), and choline chloride:PTSA (1:1 mmol) (200 mg) were further sequentially added under O_2 atm at 100 °C and maintained for 4 h. After the complete formation of cyclized product **5**, substituted benzyl alcohol **6** (0.2 mmol, 1.0 equiv), CAN (10 mol %) as a catalyst, TEMPO (10 mol %) as an oxidant, and choline chloride:PTSA (1:1 mmol) (200 mg) were added at 100 °C and maintained for 2 h. After the complete formation of alkenylated product **8** (as monitored by TLC), the reaction mixture was then diluted with water (20 mL) and the CH_2Cl_2 solvent, and the crude reaction mixture was extracted with CH_2Cl_2 (2 × 10 mL^2). The organic extracts were dried over anhydrous Na_2SO_4, and after the removal of CH_2Cl_2, the crude mixture was passed through a silica-packed column chromatograph to obtain the pure products **8a**−**8d** (73−78% yield).

Gram-Scale Experiment for the Synthesis of 7c. To a saturated ketone **1a** (1.27 g, 5.0 mmol, 1.0 equiv), CAN (548 mg, 20 mol %), TEMPO (156 mg, 20 mol %), and TBAB (2.5 g) were added in an oven-dried reaction vessel, and the mixture was allowed to stir at 100 °C for 3 h in the parallel synthesizer. After the complete formation of the dehydrogenative products as monitored by TLC, 1,3-cyclohexadione **3** (560 mg, 5.0 mmol, 1.0 equiv), NH_4OAc (3.85 g, 50.0 mmol, 10.0 equiv), and choline chloride:PTSA (1:1) were further sequentially added under O_2 atm at 100 °C and maintained for 4 h. After completion of cyclization, 4-fluoro benzyl alcohol **6b** (631 mg, 5 mmol, 1.0 equiv), CAN (274 mg, 10 mol %), TEMPO (78 mg, 10 mol %), and choline chloride:PTSA (1:1) were added at 100 °C and maintained for 2 h. After completion of the reaction (as monitored by TLC), the reaction mixture was then diluted with water (50 mL) and the CH_2Cl_2 solvent, and the crude reaction mixture was extracted with CH_2Cl_2 (2 × 50 mL^2). The organic extracts were dried over anhydrous Na_2SO_4, and after the removal of CH_2Cl_2, the crude mixture was passed through silica-packed column chromatography to obtain the pure product **7c** (72% yield).

Product Functionalization. *Synthesis of Heterocyclics Containing α-Alkenylated Dihydroquinolinone (**7p** and **7q**).* The (1,3-diphenyl-1*H*-pyrazol-4-yl)methanol[50,51] **6c** and 3-(hydroxymethyl)-4*H*-chromen-4-one[52] **6d** synthetic procedure follows the standard procedure as per the literature. To a saturated ketone **1a** (51 mg, 0.2 mmol, 1.0 equiv), CAN (22 mg, 20 mol %), TEMPO (6 mg, 20 mol %), and TBAB (100 mg) were added to an oven-dried reaction vessel, and the mixture was allowed to stir at 100 °C for 3 h in the parallel synthesizer. After the complete formation of the dehydrogenative products as monitored by TLC, 1,3-cyclohexadione **3** (22 mg, 0.2 mmol, 1.0 equiv), NH_4OAc (154 mg, 2.0 mmol, 10.0 equiv), and choline chloride:PTSA (1:1) (200 mg) were further sequentially added under O_2 atm at 100 °C and maintained for 4 h. After completion of cyclization, **6c** or **6d** (50 mg or 35 mg, 0.2 mmol, 1.0 equiv), CAN (11 mg, 10 mol %), TEMPO (3 mg, 10 mol %), and choline chloride:PTSA (1:1) (200 mg) were added at 100 °C and maintained for 2 h. After completion of the reaction (as monitored by TLC), the reaction mixture was then diluted with water (20 mL) and the CH_2Cl_2 solvent, and the crude reaction mixture was extracted with CH_2Cl_2 (2 × 10 mL^2). The organic extracts were dried over anhydrous Na_2SO_4, and after the removal of CH_2Cl_2, the crude mixture was passed through a silica-packed column chromatograph to obtain the pure product **7p** (77% yield) or **7q** (74% yield).

*Synthesis of (E)-6-(4-Fluorobenzylidene)-4-(4-methoxyphenyl)-2-(p-tolyl)-5,6,7,8-tetrahydroquinolin-5-ol (**9**).* (*E*)-6-(4-Fluorobenzylidene)-4-(4-methoxyphenyl)-2-(*p*-tolyl)-7,8-dihydroquinolin-5(6*H*)-one **7c** (90 mg, 0.2 mmol, 1.0 equiv) in 10 mL of methanol was taken in a round-bottom flask at room temperature with stirring. Sodium borohydride[45] (8 mg, 0.2 mmol, 1.0 equiv) was slowly added and maintained for 15 min at room temperature. After complete formation of the reduction product (as monitored by TLC), the crude reaction mixture was distilled out under reduced pressure. After that, the crude reaction mixture was diluted with water (20 mL) and extracted with the CH_2Cl_2 (2 × 15 mL^2) solvent. The organic extracts were dried over anhydrous Na_2SO_4, and after the evaporation of the organic solvent, they yielded 89% of the pure product **9**.

*Synthesis of 7-(4-Fluorophenyl)-1,3-bis(4-methoxyphenyl)-5,6,7,9,10,11-hexahydro-8H-chromeno[2,3-f]quinolin-8-one (**10**).* DMU:malonic acid[34] (7:3) (300 mg) was added to the reaction vessel and heated to 90 °C for 10 min. After that, α-alkenylated dihydroquinolinone **7j** (93 mg, 0.2 mmol, 1.0 equiv) and 1,3-cyclohexadione **3a** (22 mg, 0.2 mmol, 1.0 equiv) were added at 90 °C for 3 h. The reaction was monitored by TLC. After completion of the reaction, the reaction mixture was then diluted with water (20 mL) and the CH_2Cl_2 solvent, and the crude reaction mixture was extracted with CH_2Cl_2 (2 × 10 mL^2). The organic extracts were dried over anhydrous Na_2SO_4, and after the removal of CH_2Cl_2, the crude mixture was passed through a silica-packed column chromatograph to obtain the pure product **10** (82% yield).

*Synthesis of (E)-11-Benzylidene-7-(4-fluorophenyl)-15-phenyl-8,9,11,12,13,14-hexahydro-6H,7H-chromeno-[3′,4′:5,6]pyrano[2,3-a]acridin-6-one (**12**).* The DMU:malonic acid (7:3) (300 mg) DES[34] was added to the reaction vessel at 90 °C for 10 min. After that, α-alkenylated hexahydroacridinone **8a** (94 mg, 0.2 mmol, 1.0 equiv) and 4-hydroxycoumarin **11** (32 mg, 0.2 mmol, 1.0 equiv) were added at 90 °C for 4 h. The reaction was monitored by TLC. After completion of the reaction, the reaction mixture was then diluted with water (20 mL) and the CH_2Cl_2 solvent, and the crude reaction mixture was extracted with CH_2Cl_2 (2 × 10 mL^2). The organic extracts were dried over anhydrous Na_2SO_4, and after the removal of CH_2Cl_2, the crude mixture was passed through a silica-packed column chromatograph to obtain the pure product **12** (85%).

Characterization Data for Starting Materials and Control Experiment Intermediates. *3-(4-Methoxyphenyl)-1-(p-tolyl)propan-1-one (**1a**).* The synthetic procedure follows the standard procedure as per the literature.[34] White solid (216 mg, 85% yield), **Mp:** 58−60 °C, R_f = 0.8 (5% ethyl acetate in petroleum ether); **^{1}H NMR** (400 MHz, $CDCl_3$) δ 7.89 (d, *J* = 8.2 Hz, 2H), 7.27 (d, *J* = 8.1 Hz, 2H), 7.20 (d, *J* = 8.6 Hz, 2H), 6.87 (d, *J* = 8.6 Hz, 2H), 3.81 (s, 3H), 3.27 (t, *J* = 7.7 Hz, 2H), 3.03 (t, *J* = 7.7 Hz, 2H), 2.43 (s, 3H). **^{13}C NMR**

https://doi.org/10.1021/acsomega.4c02058
ACS Omega 2024, 9, 36198−36219

(101 MHz, $CDCl_3$) δ 199.08, 158.00, 143.79, 134.49, 133.45, 129.35, 129.28, 128.18, 113.96, 55.28, 40.60, 29.40, 21.62. **FT-IR:** ν = 2997, 2923, 2836, 1674, 1603, 1513, 1272, 1243, 1181, 1033, 805, 522 cm^{-1}. **GC-MS** (m/z): calculated for $C_{17}H_{19}O_2$: 254.1307; found: 254.143.

*2,6-Dibenzylcyclohexan-1-one (**2a**).* The synthetic procedure follows the standard procedure as per the literature.[53] White solid (462 mg, 83% yield), **Mp:** 114−115 °C, R_f = 0.8 (5% ethyl acetate in petroleum ether); **^{1}H NMR** (400 MHz, $CDCl_3$) δ 7.27 (t, J = 7.3 Hz, 4H), 7.17 (dd, J = 14.6, 7.2 Hz, 6H), 3.23 (dd, J = 13.9, 4.7 Hz, 2H), 2.57 (td, J = 13.1, 5.1 Hz, 2H), 2.42 (dd, J = 13.9, 8.6 Hz, 2H), 2.10−2.00 (m, 2H), 1.82−1.72 (m, 1H), 1.53 (m, 1H), 1.34 (m, 2H). **^{13}C NMR** (101 MHz, $CDCl_3$) δ 212.86, 140.61, 129.18, 128.29, 125.93, 52.91, 35.51, 34.88, 25.37. **GC-MS** (m/z): calculated for $C_{20}H_{22}O$: 278.395; found: 278.330.

*3-(Hydroxymethyl)-4H-chromen-4-one (**6d**).* The 3-(hydroxymethyl)-4*H*-chromen-4-one **6d** synthetic procedure follows the standard procedure as per the literature.[52] White solid (137 mg, 82% yield), **Mp:** 108−110 °C, R_f = 0.2 (10% ethyl acetate in petroleum ether); **^{1}H NMR** (400 MHz, $CDCl_3$) δ 8.22 (d, J = 7.6 Hz, 1H), 7.95 (s, 1H), 7.68 (t, J = 7.5 Hz, 1H), 7.50−7.37 (m, 2H), 4.59 (s, 2H), 3.15 (s, 1H). **^{13}C NMR** (101 MHz, $CDCl_3$) δ 178.52, 156.62, 152.89, 133.95, 125.62, 125.30, 123.83, 123.31, 118.25, 58.58.

*4-(4-Methoxyphenyl)-2-(p-tolyl)-4,6,7,8-tetrahydro-5H-chromen-5-one (**13**).* The synthetic procedure follows the standard procedure as per the literature.[54] White solid, R_f = 0.5 (10% ethyl acetate in petroleum ether); **^{1}H NMR** (400 MHz, $CDCl_3$) δ 7.51 (d, J = 8.2 Hz, 2H), 7.28 (d, J = 8.4 Hz, 2H), 7.20 (d, J = 8.1 Hz, 2H), 6.85 (d, J = 8.6 Hz, 2H), 5.67 (d, J = 5.0 Hz, 1H), 4.49 (d, J = 5.0 Hz, 1H), 3.79 (s, 3H), 2.78−2.62 (m, 2H), 2.49−2.32 (m, 5H), 2.15−1.96 (m, 2H). **^{13}C NMR** (101 MHz, $CDCl_3$) δ 197.55, 166.13, 158.22, 146.82, 138.69, 137.75, 130.26, 129.25, 129.12, 124.39, 114.13, 113.76, 103.78, 55.24, 37.15, 34.36, 27.78, 21.26, 20.47.

*(E)-3-(4-Methoxyphenyl)-1-(p-tolyl)prop-2-en-1-one (**1a′**).* The intermediate **1a′** was isolated from the control experiment study and conformed by NMR. White solid (48 mg, 95%), R_f = 0.6 (10% ethyl acetate in petroleum ether); **^{1}H NMR** (400 MHz, $CDCl_3$) δ 7.93 (d, J = 8.2 Hz, 2H), 7.78 (d, J = 15.6 Hz, 1H), 7.60 (d, J = 8.7 Hz, 2H), 7.42 (d, J = 15.6 Hz, 1H), 7.30 (d, J = 8.0 Hz, 2H), 6.94 (d, J = 8.8 Hz, 2H), 3.86 (s, 3H), 2.44 (s, 3H). **^{13}C NMR** (101 MHz, $CDCl_3$) δ 190.10, 161.60, 144.26, 143.37, 135.93, 130.17, 129.28, 128.58, 127.77, 119.84, 114.41, 55.42, 21.67.

*2,6-Di((E)-benzylidene)cyclohexan-1-one (**2a′**).* The intermediate **2a′** was isolated from the control experiment study and conformed by NMR;. Yellow solid (51 mg, 93%), **Mp:** 117−118 °C, R_f = 0.5 (5% ethyl acetate in petroleum ether); **^{1}H NMR** (400 MHz, $CDCl_3$) δ 7.81 (s, 2H), 7.47 (d, J = 7.4 Hz, 4H), 7.41 (t, J = 7.4 Hz, 4H), 7.38−7.31 (m, 2H), 2.97−2.91 (m, 4H), 1.85−1.75 (m, 2H). **^{13}C NMR** (101 MHz, $CDCl_3$) δ 190.42, 136.96, 136.22, 136.01, 130.38, 128.60, 128.40, 28.47, 23.04. **GC-MS** (m/z): calculated for $C_{20}H_{18}O$: 274.3630; found: 274.6222.

Characterization Data for the Synthesized Products. *4-(4-Methoxyphenyl)-2-(p-tolyl)-7,8-dihydroquinolin-5(6H)-one (**4a**).* White solid (58 mg, 85% yield), **Mp:** 115−117 °C, R_f = 0.6 (10% ethyl acetate in petroleum ether); **^{1}H NMR** (400 MHz, $CDCl_3$) δ 7.97 (d, J = 8.2 Hz, 2H), 7.48 (s, 1H), 7.29 (d, J = 8.0 Hz, 2H), 7.25−7.22 (m, 2H), 6.95 (dd, J = 8.7 Hz, 2H), 3.86 (s, 3H), 3.26 (t, J = 6.2 Hz, 2H), 2.72−2.63 (t, J = 6.2 Hz, 2H), 2.41 (s, 3H), 2.27−2.16 (m, 2H). **^{13}C NMR** (101 MHz, $CDCl_3$) δ 198.05, 165.00, 159.45, 158.94, 152.23, 140.25, 135.48, 132.72, 129.62, 129.30, 127.36, 124.73, 121.71, 113.55, 55.31, 40.22, 34.05, 21.67, 21.41. **FT-IR:** ν = 3013, 2950, 2831, 1678, 1532, 1507, 1236, 1177, 1028, 826, 526, 488 cm^{-1}. **GC-MS** (EI) (m/z): [M] calculated for $C_{23}H_{21}NO_2$: 343.1572; found: 343.356.

*2,4-Bis(4-methoxyphenyl)-7,8-dihydroquinolin-5(6H)-one (**4b**).* Pale-yellow solid (60 mg, 83% yield), **Mp:** 118−119 °C, R_f = 0.6 (10% ethyl acetate in petroleum ether); **^{1}H NMR** (400 MHz, $CDCl_3$) δ 8.07 (d, J = 7.8 Hz, 2H), 7.47 (s, 1H), 7.27 (d, J = 10.3 Hz, 2H), 7.00 (dd, J = 15.5, 8.1 Hz, 4H), 3.89 (s, 6H), 3.27 (s, 2H), 2.70 (s, 2H), 2.23 (s, 2H). **^{13}C NMR** (101 MHz, $CDCl_3$) δ 197.96, 165.00, 161.33, 159.43, 158.50, 152.20, 132.81, 130.81, 129.27, 128.92, 124.36, 121.18, 114.25, 113.54, 55.42, 55.31, 40.20, 34.07, 21.67. **FT-IR:** ν = 2996, 2937, 2839, 1680, 1577, 1532, 1233, 1174, 1031, 830, 558, 529 cm^{-1}. **GC-MS** (EI) (m/z): [M] calculated for $C_{23}H_{21}NO_3$: 359.1521; found: 359.232.

*4-Phenyl-2-(p-tolyl)-7,8-dihydroquinolin-5(6H)-one (**4c**).* White solid (53 mg, 84% yield), **Mp:** 130−132 °C, R_f = 0.7 (10% ethyl acetate in petroleum ether); **^{1}H NMR** (400 MHz, $CDCl_3$) δ 8.00 (d, J = 7.7 Hz, 2H), 7.52 (s, 1H), 7.44 (s, 3H), 7.30 (t, J = 5.6 Hz, 4H), 3.31 (s, 2H), 2.70 (s, 2H), 2.44 (s, 3H), 2.25 (s, 2H). **^{13}C NMR** (101 MHz, $CDCl_3$) δ 197.77, 164.91, 159.00, 152.53, 140.70, 140.32, 135.39, 129.63, 128.03, 127.75, 127.72, 127.38, 124.64, 121.56, 40.11, 34.01, 21.68, 21.40. **FT-IR:** ν = 3053, 2937, 2871.49, 1685, 1577, 1526, 1360, 1230, 1175, 1016, 816, 760, 696, 514 cm^{-1}. **GC-MS** (EI) (m/z): [M] calculated for $C_{22}H_{19}NO$: 313.1467; found: 313.188.

*2-(4-Bromophenyl)-4-(4-methoxyphenyl)-7,8-dihydroquinolin-5(6H)-one (**4d**).* Pale-yellow solid (73 mg, 89% yield), **Mp:** 142−144 °C, R_f = 0.7 (10% ethyl acetate in petroleum ether); **^{1}H NMR** (400 MHz, $CDCl_3$) δ 7.86 (d, J = 8.6 Hz, 2H), 7.51 (d, J = 8.6 Hz, 2H), 7.39 (s, 1H), 7.14 (d, J = 8.7 Hz, 2H), 6.87 (t, J = 8.7 Hz, 2H), 3.77 (s, 3H), 3.17 (t, J = 6.2 Hz, 2H), 2.60 (t, J = 6.4 Hz, 2H), 2.18−2.06 (m, 2H). **^{13}C NMR** (101 MHz, $CDCl_3$) δ 197.85, 165.08, 159.59, 157.56, 152.52, 137.11, 132.39, 132.03, 129.31, 128.98, a125.20, 124.64, 121.70, 113.62, 55.32, 40.20, 33.99, 21.61. **FT-IR:** ν = 2932.23, 2824.24, 1680.66, 1529.27, 1509.99, 1243.86, 1175.40, 1007.62, 821.53, 528.40 cm^{-1}. **GC-MS** (EI) (m/z): [M] calculated for $C_{22}H_{18}BrNO_2$: 407.0521; found: 407.078.

*2,4-Bis(4-fluorophenyl)-7,7-dimethyl-7,8-dihydroquinolin-5(6H)-one (**4e**).* Pale-yellow solid (62 mg, 86% yield), **Mp:** 185−187 °C, R_f = 0.65 (10% ethyl acetate in petroleum ether); **^{1}H NMR** (400 MHz, $CDCl_3$) δ 8.08 (dd, J = 8.6, 5.5 Hz, 2H), 7.43 (s, 1H), 7.26−7.21 (dd, J = 5.4 Hz, 2H), 7.16 (t, J = 8.6 Hz, 2H), 7.11 (t, J = 8.6 Hz, 2H), 3.18 (s, 2H), 2.54 (s, 2H), 1.16 (s, 6H). **^{13}C NMR** (101 MHz, $CDCl_3$) δ 197.79, 165.45, 163.81, 163.72, 162.96, 161.35, 158.32, 151.32, 136.18, 136.15, 134.24, 134.20, 129.66, 129.58, 129.48, 129.39, 123.71, 121.40, 116.01, 115.79, 115.18, 114.96, 53.82, 47.83, 32.59, 28.27. **FT-IR:** ν = 2962, 2921, 1687, 1534, 1501, 1274, 1221, 1158, 836, 544 cm^{-1}. **GC-MS** (EI) (m/z): [M] calculated for $C_{23}H_{19}F_2NO$: 363.1435; found: 363.132.

*4-(4-Methoxyphenyl)-7,7-dimethyl-2-(p-tolyl)-7,8-dihydroquinolin-5(6H)-one (**4f**).* White solid (63 mg, 85% yield), **Mp:** 121−123 °C, R_f = 0.5 (10% ethyl acetate in petroleum ether); **^{1}H NMR** (400 MHz, $CDCl_3$) δ 7.98 (d, J = 8.1 Hz, 2H), 7.48 (s, 1H), 7.29 (d, J = 8.0 Hz, 2H), 7.24 (d, J = 8.7 Hz, 2H), 6.96 (d, J = 8.7 Hz, 2H), 3.86 (s, 3H), 3.18 (s, 2H),

https://doi.org/10.1021/acsomega.4c02058
ACS Omega 2024, 9, 36198−36219

2.55 (s, 2H), 2.42 (s, 3H), 1.16 (s, 6H). **^{13}C NMR** (101 MHz, $CDCl_3$) δ 198.10, 163.57, 159.45, 159.29, 151.84, 140.22, 135.49, 132.63, 129.61, 129.36, 127.35, 123.70, 121.56, 113.54, 55.32, 53.97, 47.93, 32.62, 28.32, 21.40. **FT-IR:** ν = 2955, 2927, 1692, 1531, 1503, 1295, 1243, 1174, 1037, 828, 553 cm^{-1}. **GC-MS** (EI) (m/z): [M] calculated for $C_{25}H_{25}NO_2$: 371.1885; found: 371.279.

*2,4-Bis(4-methoxyphenyl)-7,7-dimethyl-7,8-dihydroquinolin-5(6H)-one (**4g**).* Pale-yellow solid (63 mg, 81% yield), **Mp:** 206−207 °C, R_f = 0.45 (10% ethyl acetate in petroleum ether); **^{1}H NMR** (400 MHz, $CDCl_3$) δ 8.05 (d, J = 8.7 Hz, 2H), 7.44 (s, 1H), 7.24 (d, J = 8.6 Hz, 2H), 6.98 (dd, J = 15.1, 8.8 Hz, 4H), 3.86 (d, J = 2.6 Hz, 6H), 3.17 (s, 2H), 2.54 (s, 2H), 1.16 (s, 6H). **^{13}C NMR** (101 MHz, $CDCl_3$) δ 198.01, 163.57, 161.33, 159.44, 158.86, 151.81, 132.71, 130.82, 129.34, 128.91, 123.34, 121.04, 114.25, 113.52, 55.41, 55.32, 53.95, 47.94, 32.59, 28.32. **FT-IR:** ν = 2959, 1675, 1511, 1526, 1240, 1171, 1027, 825, 539 cm^{-1}. **GC-MS** (EI) (m/z): [M] calculated for $C_{25}H_{25}NO_3$: 387.1834; found: 387. 5448.

*Ethyl 4-(4-methoxyphenyl)-2-methyl-6-(p-tolyl)nicotinate (**4h**).* Colorless liquid (59 mg, 82% yield), R_f = 0.7 (10% ethyl acetate in petroleum ether); **^{1}H NMR** (400 MHz, $CDCl_3$) δ 7.84 (d, J = 8.2 Hz, 2H), 7.43 (s, 1H), 7.29 (dd, J = 8.8 Hz, 2H), 7.18 (d, J = 8 Hz, 2H), 6.88 (dd, J = 8.8 Hz, 2H), 4.08 (q, J = 7.1 Hz, 2H), 3.76 (s, 3H), 2.61 (s, 3H), 2.32 (s, 3H), 1.01 (t, J = 7.1 Hz, 3H). **^{13}C NMR** (101 MHz, $CDCl_3$) δ 169.36, 159.98, 157.34, 155.52, 148.36, 139.33, 136.16, 131.32, 129.50, 129.24, 127.07, 126.49, 114.16, 114.06, 61.31, 55.37, 23.16, 21.32, 13.86. **FT-IR:** ν = 2952, 2833, 1682, 1577, 1509, 1253, 1157, 1097, 1021, 822, 595, 511 cm^{-1}. **GC-MS** (EI) (m/z): [M] calculated for $C_{23}H_{23}NO_3$: 361.1678; found: 361.175.

*(E)-5-Benzylidene-9-phenyl-3,4,5,6,7,8-hexahydroacridin-1(2H)-one (**5a**).* White solid (61 mg, 83% yield), **Mp:** 228−230 °C, R_f = 0.6 (10% ethyl acetate in petroleum ether); **^{1}H NMR** (400 MHz, $CDCl_3$) δ 8.12 (s, 1H), 7.49−7.33 (m, 7H), 7.29 (d, J = 8.0 Hz, 1H), 7.05 (t, J = 8 Hz, 2H), 3.22 (t, J = 6.2 Hz, 2H), 2.85 (t, J = 6.0 Hz, 2H), 2.58 (t, J = 6.8 Hz, 2H), 2.39 (t, J = 6.1 Hz, 2H), 2.21−2.10 (m, 2H), 1.75−1.65 (m, 2H). **^{13}C NMR** (101 MHz, $CDCl_3$) δ 197.93, 161.31, 155.56, 150.99, 139.42, 137.61, 135.75, 130.75, 130.52, 129.82, 128.31, 128.18, 127.24, 126.96, 126.93, 124.55, 40.37, 33.95, 27.62, 27.48, 22.70, 21.72. **FT-IR:** ν = 2923, 2909, 2846, 1675, 1530, 1351, 1270, 930, 762, 696, 522 cm^{-1}. **HRMS** (ESI) (m/z): [M + H]$^+$ calculated for $C_{26}H_{24}NO^+$: 366.1854; found: 366.1857.

*(E)-5-(2-Chlorobenzylidene)-9-(2-chlorophenyl)-3,4,5,6,7,8-hexahydroacridin-1(2H)-one (**5b**).* White solid (70 mg, 81% yield), **Mp:** 195−197 °C, R_f = 0.7 (10% ethyl acetate in petroleum ether); **^{1}H NMR** (400 MHz, $CDCl_3$) δ 8.26 (s, 1H), 7.47 (d, J = 8.7 Hz, 2H), 7.41−7.32 (t, J = 9.6 Hz, 3H), 7.28 (d, J = 12 Hz, 2H), 7.03 (d, J = 2.8 Hz, 1H), 3.27 (s, 2H), 2.77−2.56 (m, 4H), 2.40 (s, 2H), 2.20 (s, 2H), 1.76 (s, 2H). **^{13}C NMR** (101 MHz, $CDCl_3$) δ 197.73, 161.53, 155.40, 147.98, 138.26, 137.20, 136.05, 134.61, 131.44, 130.83, 130.42, 129.51, 129.35, 128.58, 128.25, 127.84, 126.96, 126.20, 124.58, 39.98, 33.83, 27.44, 26.87, 22.55, 21.67. **FT-IR:** ν = 2950, 2855, 1674, 1534, 1434, 1273, 1033, 736, 700, 542 cm^{-1}. **HRMS** (ESI) (m/z): [M + H]$^+$ calculated for $C_{26}H_{22}Cl_2NO^+$: 434.1078; found: 434.1083.

*(E)-9-(Furan-2-yl)-5-(furan-2-ylmethylene)-3,4,5,6,7,8-hexahydroacridin-1(2H)-one (**5c**).* Green solid (49 mg, 71% yield), **Mp:** 245−248 °C, R_f = 0.75 (10% ethyl acetate in petroleum ether); **^{1}H NMR** (400 MHz, $CDCl_3$) δ 7.95 (s, 1H), 7.53 (d, J = 12.0 Hz, 2H), 6.64−6.45 (m, 3H), 6.33 (d, J = 3.1 Hz, 1H), 3.16 (t, J = 6.1 Hz, 2H), 3.00 (t, J = 5.6 Hz, 2H), 2.71−2.59 (m, 4H), 2.23−2.10 (m, 2H), 1.89−1.76 (m, 2H). **^{13}C NMR** (101 MHz, CDCl3) δ 197.42, 161.35, 155.93, 153.77, 149.05, 143.02, 142.38, 138.06, 132.80, 131.64, 125.36, 118.38, 112.91, 111.96, 110.90, 109.52, 39.97, 33.61, 27.86, 26.92, 22.02, 21.70. **FT-IR:** ν = 2918, 2846, 1514, 1448, 1264, 1133, 1018, 767, 679, 566 cm^{-1}. **HRMS** (ESI) (m/z): [M + H]$^+$ calculated for $C_{22}H_{20}NO_3^+$: 346.1443; found: 346.1441.

*(E)-6-Benzylidene-4-(4-methoxyphenyl)-2-(p-tolyl)-7,8-dihydroquinolin-5(6H)-one (**7a**).* Pale-yellow solid (68 mg, 79% yield), **Mp:** 120−123 °C, R_f = 0.55 (10% ethyl acetate in petroleum ether); **^{1}H NMR** (400 MHz, $CDCl_3$) δ 8.00 (d, J = 8.2 Hz, 2H), 7.79 (s, 1H), 7.58 (s, 1H), 7.49−7.39 (m, 4H), 7.39−7.28 (m, 5H), 6.99 (d, J = 8.7 Hz, 2H), 3.87 (s, 3H), 3.23 (s, 4H), 2.42 (s, 3H). **^{13}C NMR** (101 MHz, $CDCl_3$) δ 187.26, 163.53, 159.58, 158.94, 152.51, 140.26, 136.92, 135.74, 135.66, 135.56, 132.50, 130.00, 129.64, 129.42, 128.77, 128.53, 127.36, 125.52, 121.85, 113.76, 55.30, 32.84, 25.91, 21.42. **FT-IR:** ν = 2952, 2907, 2835, 1671, 1576, 1509, 1244, 1177, 822, 692, 537 cm^{-1}. **HRMS** (ESI) (m/z): [M + H]$^+$ calculated for $C_{30}H_{26}NO_2^+$: 432.1964; found: 432.1844.

*(E)-6-(4-Methoxybenzylidene)-4-(4-methoxyphenyl)-2-(p-tolyl)-7,8-dihydroquinolin-5(6H)-one (**7b**).* Pale-yellow solid (74 mg, 80% yield), **Mp:** 135−137 °C, R_f = 0.4 (10% ethyl acetate in petroleum ether); **^{1}H NMR** (400 MHz, $CDCl_3$) δ 8.00 (d, J = 7.4 Hz, 2H), 7.75 (s, 1H), 7.57 (s, 1H), 7.45 (d, J = 7.4 Hz, 2H), 7.31 (d, J = 6.0 Hz, 4H), 6.97 (t, J = 8.6 Hz, 4H), 3.86 (s, 6H), 3.23 (s, 4H), 2.42 (s, 3H). **^{13}C NMR** (101 MHz, $CDCl_3$) δ 187.32, 163.36, 160.13, 159.53, 158.78, 152.30, 140.16, 136.84, 135.63, 133.71, 132.54, 131.89, 129.62, 129.42, 128.31, 127.33, 125.72, 121.81, 114.04, 113.73, 55.37, 55.28, 32.78, 25.94, 21.40. **FT-IR:** ν = 2961, 2836, 1665, 1579, 1506, 1247, 1176, 1021, 816, 538 cm^{-1}. **HRMS** (ESI) (m/z): [M + H]$^+$ calculated for $C_{31}H_{28}NO_3^+$: 462.2069; found: 462.1986.

*(E)-6-(4-Fluorobenzylidene)-4-(4-methoxyphenyl)-2-(p-tolyl)-7,8-dihydroquinolin-5(6H)-one (**7c**).* Yellow solid (67 mg, 74% yield), **Mp:** 128−131 °C, R_f = 0.55 (10% ethyl acetate in petroleum ether); **^{1}H NMR** (400 MHz, $CDCl_3$) δ 8.00 (d, J = 7.7 Hz, 2H), 7.74 (s, 1H), 7.58 (s, 1H), 7.45 (t, J = 8.0 Hz, 2H), 7.31 (t, J = 6.5 Hz, 4H), 7.12 (t, J = 8.3 Hz, 2H), 6.99 (d, J = 8.1 Hz, 2H), 3.87 (s, 3H), 3.21 (s, 4H), 2.42 (s, 3H). **^{13}C NMR** (101 MHz, $CDCl_3$) δ 187.07, 163.39, 159.60, 158.98, 152.52, 140.28, 135.69, 135.53, 135.43, 132.45, 131.91, 131.83, 129.63, 129.40, 127.36, 125.45, 121.84, 115.77, 115.55, 113.76, 55.28, 32.75, 25.83, 21.39. **FT-IR:** ν = 2923, 2826, 1676, 1607, 1536, 1503, 1226, 1179, 954, 824, 579, 527, 496 cm^{-1}. **HRMS** (ESI) (m/z): [M + H]$^+$ calculated for $C_{30}H_{25}FNO_2^+$: 450.1869; found: 450.1912.

*(E)-6-(2-Fluorobenzylidene)-4-(4-methoxyphenyl)-2-(p-tolyl)-7,8-dihydroquinolin-5(6H)-one (**7d**).* Yellow solid (66 mg, 73% yield), **Mp:** 123−125 °C, R_f = 0.54 (10% ethyl acetate in petroleum ether); **^{1}H NMR** (400 MHz, $CDCl_3$) δ 8.00 (d, J = 8.1 Hz, 2H), 7.80 (s, 1H), 7.58 (s, 1H), 7.35−7.20 (m, 6H), 7.19 (t, J = 7.5 Hz, 1H), 7.12 (t, J = 9.2 Hz, 1H), 6.99 (d, J = 8.6 Hz, 2H), 3.87 (s, 3H), 3.23 (t, J = 6.4 Hz, 2H), 3.11 (t, J = 6.1 Hz, 2H), 2.42 (s, 3H). **^{13}C NMR** (101 MHz, $CDCl_3$) δ 186.60, 163.77, 161.98, 159.60, 158.99, 152.83, 140.31, 137.71, 135.49, 132.55, 130.63, 130.60, 130.51, 130.42, 129.63, 129.39, 127.39, 125.23, 123.91, 123.87, 123.71, 121.89, 116.02, 115.80, 113.74, 55.29, 32.90, 26.24, 21.39. **FT-IR:** ν = 2922, 2824, 1673, 1604, 1535, 1505, 1224, 1179, 1040, 955,

https://doi.org/10.1021/acsomega.4c02058
ACS Omega 2024, 9, 36198−36219

823, 527, 496, 476 cm^{-1}. **HRMS** (ESI) (m/z): $[M + H]^+$ calculated for $C_{30}H_{25}FNO_2^+$: 450.1869; found: 450.1872.

*(E)-6-(2-Chlorobenzylidene)-4-(4-methoxyphenyl)-2-(p-tolyl)-7,8-dihydroquinolin-5(6H)-one (**7e**).* Pale-yellow solid (72 mg, 77% yield), **Mp:** 137−138 °C, R_f = 0.6 (10% ethyl acetate in petroleum ether); **^{1}H NMR** (400 MHz, $CDCl_3$) δ 7.95 (d, J = 4.4 Hz, 2H), 7.89 (s, 1H), 7.58 (s, 1H), 7.44 (s, 1H), 7.33 (d, J = 20.2 Hz, 7H), 7.00 (s, 2H), 3.87 (s, 3H), 3.22 (s, 2H), 3.09 (s, 2H), 2.42 (s, 3H). **^{13}C NMR** (101 MHz, $CDCl_3$) δ 186.65, 163.81, 159.56, 159.05, 152.93, 140.34, 137.14, 135.48, 135.04, 134.34, 133.82, 132.63, 130.30, 129.86, 129.71, 129.65, 129.34, 127.39, 126.41, 125.16, 121.95, 113.73, 55.30, 33.07, 26.03, 21.42. **FT-IR:** ν = 2922, 2857, 1667, 1577, 1532, 1245, 1178, 823, 760, 547 cm^{-1}. **HRMS** (ESI) (m/z): $[M + H]^+$ calculated for $C_{30}H_{25}ClNO_2^+$: 466.1574; found: 466.1461.

*(E)-6-(2,4-Dichlorobenzylidene)-4-(4-methoxyphenyl)-2-(p-tolyl)-7,8-dihydroquinolin-5(6H)-one (**7f**).* Dark-yellow solid (72 mg, 72% yield), **Mp:** 144−146 °C, R_f = 0.7 (10% ethyl acetate in petroleum ether); **^{1}H NMR** (400 MHz, $CDCl_3$) δ 8.00 (d, J = 7.6 Hz, 2H), 7.80 (s, 1H), 7.58 (s, 1H), 7.47 (s, 1H), 7.30 (s, 6H), 6.99 (d, J = 7.9 Hz, 2H), 3.87 (s, 3H), 3.23 (d, J = 5.2 Hz, 2H), 3.06 (s, 2H), 2.42 (s, 3H). **^{13}C NMR** (101 MHz, $CDCl_3$) δ 186.37, 163.68, 159.61, 159.14, 152.98, 140.40, 137.67, 135.79, 135.42, 134.90, 132.88, 132.54, 130.97, 129.78, 129.64, 129.33, 127.40, 126.84, 125.04, 121.96, 113.75, 55.29, 32.95, 26.06, 21.40. **FT-IR:** ν = 2956, 2915, 2845, 1674, 1581, 1527, 1469, 1245, 1175, 1027, 956, 823, 574 cm^{-1}. **HRMS** (ESI) (m/z): $[M + H]^+$ calculated for $C_{30}H_{24}Cl_2NO_2^+$: 500.1184; found: 500.1251.

*(E)-6-(2,4-Dichlorobenzylidene)-4-phenyl-2-(p-tolyl)-7,8-dihydroquinolin-5(6H)-one (**7g**).* Yellow solid (74 mg, 79% yield), **Mp:** 148−151 °C, R_f = 0.7 (10% ethyl acetate in petroleum ether); **^{1}H NMR** (400 MHz, $CDCl_3$) δ 8.01 (d, J = 8.2 Hz, 2H), 7.78 (s, 1H), 7.59 (s, 1H), 7.45 (d, J = 8.0 Hz, 3H), 7.39−7.33 (m, 3H), 7.30 (dd, J = 4.5, 3.4 Hz, 4H), 3.25 (t, J = 6.88 Hz, 2H), 3.07 (m, 2H), 2.42 (s, 3H). **^{13}C NMR** (101 MHz, $CDCl_3$) δ 186.22, 163.64, 159.22, 153.29, 140.52, 137.46, 135.80, 135.31, 134.93, 132.83, 132.70, 130.99, 129.78, 129.68, 128.80, 128.22, 127.93, 127.80, 127.42, 126.84, 124.98, 121.89, 32.96, 26.11, 21.43. **FT-IR:** ν = 2944, 2841, 1672, 1582, 1530, 1280, 1184, 1133, 825, 695, 577 cm^{-1}. **HRMS** (ESI) (m/z): $[M + H]^+$ calculated for $C_{29}H_{22}Cl_2NO^+$: 470.1078; found: 470.0982.

*(E)-6-(4-Methoxybenzylidene)-2,4-bis(4-methoxyphenyl)-7,8-dihydroquinolin-5(6H)-one (**7h**).* Yellow solid (74 mg, 78% yield), **Mp:** 158−159 °C, R_f = 0.4 (10% ethyl acetate in petroleum ether); **^{1}H NMR** (400 MHz, $CDCl_3$) δ 8.07 (d, J = 7.9 Hz, 2H), 7.74 (s, 1H), 7.53 (s, 1H), 7.45 (d, J = 7.7 Hz, 2H), 7.31 (d, J = 7.7 Hz, 2H), 6.98 (dd, J = 20.1, 9.1 Hz, 6H), 3.87 (d, J = 3.5 Hz, 9H), 3.22 (d, J = 6.3 Hz, 4H). **^{13}C NMR** (101 MHz, $CDCl_3$) δ 187.24, 163.37, 161.28, 160.11, 159.51, 158.36, 152.29, 136.75, 133.74, 132.63, 131.87, 130.97, 129.38, 128.89, 128.34, 125.34, 121.29, 114.26, 114.04, 113.71, 55.42, 55.37, 55.28, 32.81, 25.94. **FT-IR:** ν = 2954, 2837, 1658, 1582, 1507, 1243, 1173, 1022, 829, 532 cm^{-1}. **HRMS** (ESI) (m/z): $[M + H]^+$ calculated for $C_{31}H_{28}NO_4^+$: 478.2018; found: 478.1923.

*(E)-6-(3,4-Dimethoxybenzylidene)-2,4-bis(4-methoxyphenyl)-7,8-dihydroquinolin-5(6H)-one (**7i**).* Yellow solid (85 mg, 84% yield), **Mp**: 175−177 °C, R_f = 0.4 (10% ethyl acetate in petroleum ether); **^{1}H NMR** (400 MHz, $CDCl_3$) δ 8.07 (d, J = 8.7 Hz, 2H), 7.73 (s, 1H), 7.54 (s, 1H), 7.31 (d, J = 8.5 Hz, 2H), 7.11 (d, J = 8.2 Hz, 1H), 6.99 (dd, J = 11.3, 9.0 Hz, 5H), 6.92 (d, J = 8.3 Hz, 1H), 3.92 (d, J = 8.8 Hz, 6H), 3.87 (d, J = 3.7 Hz, 6H), 3.25 (d, J = 4.5 Hz, 2H), 3.22 (d, J = 3.8 Hz, 2H). **^{13}C NMR** (101 MHz, $CDCl_3$) δ 187.19, 163.34, 161.30, 159.53, 158.40, 152.26, 149.77, 148.79, 136.91, 134.05, 132.56, 130.94, 129.41, 128.89, 128.61, 125.32, 123.50, 121.29, 114.27, 113.72, 113.28, 110.99, 55.97, 55.43, 55.29, 32.79, 25.99. **FT-IR:** ν = 2964, 2834, 1665, 1510, 1442, 1241, 1170, 1026, 836, 575 cm^{-1}. **HRMS** (ESI) (m/z): $[M + H]^+$ calculated for $C_{32}H_{30}NO_5^+$: 508.2124; found: 508.2135.

*(E)-6-(4-Fluorobenzylidene)-2,4-bis(4-methoxyphenyl)-7,8-dihydroquinolin-5(6H)-one (**7j**).* Yellow solid (72 mg, 77% yield), **Mp:** 148−150 °C, R_f = 0.6 (10% ethyl acetate in petroleum ether); **^{1}H NMR** (400 MHz, $CDCl_3$) δ 8.08 (d, J = 8.8 Hz, 2H), 7.73 (s, 1H), 7.54 (s, 1H), 7.44 (dd, J = 8.5, 5.5 Hz, 2H), 7.31 (d, J = 8.6 Hz, 2H), 7.11 (t, J = 8.6 Hz, 2H), 7.00 (t, J = 9.3 Hz, 4H), 3.87 (d, J = 3.1 Hz, 6H), 3.20 (s, 4H). **^{13}C NMR** (101 MHz, $CDCl_3$) δ 187.02, 163.97, 163.41, 161.49, 161.36, 159.56, 158.56, 152.49, 135.63, 135.43, 132.52, 131.92, 131.84, 130.84, 129.38, 128.93, 125.06, 121.34, 115.77, 115.55, 114.28, 113.74, 55.43, 55.29, 32.77, 25.83. **FT-IR:** ν = 2959, 2841, 1662, 1582, 1504, 1236, 1174, 1021, 831, 516 cm^{-1}. **HRMS** (ESI) (m/z): $[M + H]^+$ calculated for $C_{30}H_{25}FNO_3^+$: 466.1818; found: 466.1965.

*(E)-6-(4-Chlorobenzylidene)-2,4-bis(4-methoxyphenyl)-7,8-dihydroquinolin-5(6H)-one (**7k**).* Yellow solid (73 mg, 76% yield), **Mp:** 123−125 °C, R_f = 0.6 (10% ethyl acetate in petroleum ether); **^{1}H NMR** (400 MHz, $CDCl_3$) δ 8.08 (d, J = 8.5 Hz, 2H), 7.71 (s, 1H), 7.54 (s, 1H), 7.39 (s, 4H), 7.31 (d, J = 8.3 Hz, 2H), 7.00 (t, J = 9.1 Hz, 4H), 3.87 (d, J = 2.9 Hz, 6H), 3.20 (s, 4H). **^{13}C NMR** (101 MHz, $CDCl_3$) δ 186.90, 163.43, 161.39, 159.58, 158.61, 152.54, 136.16, 135.40, 134.64, 134.19, 132.49, 131.21, 130.81, 129.37, 128.94, 128.80, 124.99, 121.35, 114.29, 113.74, 55.43, 55.29, 32.74, 25.89. **FT-IR:** ν = 2951, 2833, 1666, 1580, 1528. 1242, 1178, 1021, 833, 570, 525 cm^{-1}. **HRMS** (ESI) (m/z): $[M + H]^+$ calculated for $C_{30}H_{25}ClNO_3^+$: 482.1523; found: 482.1526.

*(E)-6-(2-Chlorobenzylidene)-2,4-bis(4-methoxyphenyl)-7,8-dihydroquinolin-5(6H)-one (**7l**).* Yellow solid (70 mg, 73% yield), **Mp:** 105−108 °C, R_f = 0.6 (10% ethyl acetate in petroleum ether); **^{1}H NMR** (400 MHz, $CDCl_3$) δ 8.08 (d, J = 7.0 Hz, 2H), 7.89 (s, 1H), 7.54 (s, 1H), 7.44 (s, 1H), 7.31 (d, J = 19.8 Hz, 5H), 7.01 (s, 4H), 3.87 (s, 6H), 3.21 (s, 2H), 3.08 (s, 2H). **^{13}C NMR** (101 MHz, $CDCl_3$) δ 186.59, 163.82, 161.40, 159.54, 158.63, 152.90, 137.17, 135.03, 134.37, 133.73, 132.72, 130.79, 130.31, 129.85, 129.70, 129.33, 128.98, 126.41, 124.79, 121.43, 114.29, 113.72, 55.43, 55.30, 33.08, 26.04. **FT-IR:** ν = 2948, 2841, 1666, 1606, 1508, 1237, 1170, 1023, 831, 547 cm^{-1}. **HRMS** (ESI) (m/z): $[M + H]^+$ calculated for $C_{30}H_{25}ClNO_3^+$: 482.1523; found: 482.1552.

*(E)-4-(4-Methoxyphenyl)-6-((E)-3-phenylallylidene)-2-(p-tolyl)-7,8-dihydroquinolin-5(6H)-one (**7m**).* Yellow solid (71 mg, 77% yield), **Mp:** 141−143 °C, R_f = 0.6 (10% ethyl acetate in petroleum ether); **^{1}H NMR** (400 MHz, $CDCl_3$) δ 8.00 (d, J = 7.5 Hz, 2H), 7.60−7.43 (m, 4H), 7.37 (t, J = 7.0 Hz, 2H), 7.31 (t, J = 7.4 Hz, 5H), 7.17 (t, J = 12.8 Hz, 1H), 6.98 (d, J = 9.1 Hz, 3H), 3.87 (s, 3H), 3.28 (s, 2H), 3.12 (s, 2H), 2.42 (s, 3H). **^{13}C NMR** (101 MHz, $CDCl_3$) δ 186.82, 163.82, 159.54, 158.66, 152.45, 141.29, 140.19, 136.61, 136.18, 135.59, 134.91, 132.60, 129.63, 129.40, 128.84, 127.35, 127.24, 125.78, 123.55, 121.81, 113.72, 55.29, 32.73, 24.63, 21.41. **FT-IR:** ν = 2923, 2846, 1663, 1577, 1507, 1286, 1241, 1177, 970, 822, 575 cm^{-1}.

https://doi.org/10.1021/acsomega.4c02058
ACS Omega 2024, 9, 36198−36219

HRMS (ESI) (m/z): $[M + H]^+$ calculated for $C_{32}H_{28}NO_2^+$: 458.2120; found: 458.2022.

*(E)-2-(4-Bromophenyl)-6-(4-(dimethylamino)-benzylidene)-4-(4-methoxyphenyl)-7,8-dihydroquinolin-5(6H)-one (**7n**).* Red color solid (89 mg, 82% yield), **Mp:** 185−187 °C, R_f = 0.4 (10% ethyl acetate in petroleum ether); **^{1}H NMR** (400 MHz, $CDCl_3$) δ 7.97 (d, J = 8.3 Hz, 2H), 7.75 (s, 1H), 7.60 (d, J = 8.3 Hz, 2H), 7.55 (s, 1H), 7.44 (d, J = 8.5 Hz, 2H), 7.30 (d, J = 8.4 Hz, 2H), 6.96 (d, J = 8.4 Hz, 2H), 6.71 (d, J = 8.5 Hz, 2H), 3.85 (s, 3H), 3.26 (d, J = 5.6 Hz, 2H), 3.20 (d, J = 6.1 Hz, 2H), 3.02 (s, 6H). **^{13}C NMR** (101 MHz, $CDCl_3$) δ 187.20, 163.38, 159.60, 157.10, 152.24, 150.78, 138.27, 137.42, 132.37, 132.28, 132.00, 131.04, 129.46, 128.93, 126.62, 124.39, 123.39, 121.77, 113.76, 111.70, 55.29, 40.16, 32.75, 26.04. **FT-IR:** ν = 2931, 2848, 1562, 1508, 1239, 1169, 957, 825, 521 cm^{-1}. **HRMS** (ESI) (m/z): $[M + H]^+$ calculated for $C_{31}H_{28}BrN_2O_2^+$: 539.1334; found: 539.1339.

*(E)-2-(4-Bromophenyl)-6-(2,4-dichlorobenzylidene)-4-(4-methoxyphenyl)-7,8-dihydroquinolin-5(6H)-one (**7o**).* Yellow solid (88 mg, 78% yield), **Mp:** 149−151 °C, R_f = 0.6 (10% ethyl acetate in petroleum ether); **^{1}H NMR** (400 MHz, $CDCl_3$) δ 8.01 (s, 2H), 7.84 (s, 1H), 7.62 (d, J = 18.3 Hz, 3H), 7.49 (s, 1H), 7.33 (s, 4H), 7.02 (s, 2H), 3.89 (s, 3H), 3.24 (s, 2H), 3.09 (s, 2H). **^{13}C NMR** (101 MHz, $CDCl_3$) δ 186.28, 163.78, 159.74, 157.78, 153.25, 137.46, 137.05, 135.81, 135.01, 132.81, 132.07, 130.96, 129.81, 129.37, 129.00, 126.88, 125.53, 124.79, 121.99, 113.82, 55.31, 32.88, 26.00. **FT-IR:** ν = 2967, 2933, 2836, 1676, 1609, 1576, 1511, 1463, 1247, 1177, 1032, 957, 820, 573, 440 cm^{-1}. **HRMS** (ESI) (m/z): $[M + H]^+$ calculated for $C_{29}H_{21}BrCl_2NO_2^+$: 564.0133; found: 564.0118.

*(E)-6-((1,3-Diphenyl-1H-pyrazol-4-yl)methylene)-4-(4-methoxyphenyl)-2-(p-tolyl)-7,8- dihydroquinolin-5(6H)-one (**7p**).* Yellow solid (89 mg, 77% yield), **Mp:** 185−187 °C, R_f 0.3 (10% ethyl acetate in petroleum ether); **^{1}H NMR** (400 MHz, $CDCl_3$) δ 8.14 (s, 1H), 7.96 (d, J = 8.2 Hz, 2H), 7.81−7.73 (m, 3H), 7.66−7.60 (m, 2H), 7.53−7.42 (m, 3H), 7.39−7.27 (m, 4H), 7.39−7.27 (m, 4H), 6.90 (m, 2H), 3.79 (s, 3H), 3.25 (t, J = 6.3 Hz, 2H), 3.16 (t, J = 6.5 Hz, 2H), 2.37 (s, 3H). **^{13}C NMR** (101 MHz, $CDCl_3$) δ 186.38, 163.28, 159.52, 158.80, 154.68, 152.45, 140.22, 139.66, 135.59, 133.91, 132.60, 132.24, 129.63, 129.58, 129.31, 128.77, 128.66, 128.51, 127.67, 127.34, 127.20, 127.12, 125.63, 121.90, 119.18, 117.10, 113.75, 55.24, 32.60, 26.36, 21.39. **FT-IR:** ν = 3127, 2943, 2839, 1658, 1583, 1509, 1249, 1180, 1026, 950, 757, 689, 567, 515 cm^{-1}. **HRMS** (ESI) (m/z): $[M + H]^+$ calculated for $C_{39}H_{32}N_3O_2^+$: 574.2495; found: 574.2558.

*(E)-4-(4-Methoxyphenyl)-6-((4-oxo-4H-chromen-3-yl)-methylene)-2-(p-tolyl)-7,8-dihydroquinolin-5(6H)-one (**7q**).* Yellow solid (74 mg, 74% yield), **Mp:** 179−181 °C, R_f = 0.2 (10% ethyl acetate in petroleum ether); **^{1}H NMR** (400 MHz, $CDCl_3$) δ 8.28 (dd, J = 8.0, 1.2 Hz, 1H), 8.04 (s, 1H), 8.01 (s, 1H), 7.99 (s, 1H), 7.75−7.62 (m, 2H), 7.57 (s, 1H), 7.52−7.41 (m, 2H), 7.30 (t, J = 7.6 Hz, 4H), 6.98 (d, J = 8.6 Hz, 2H), 3.87 (s, 3H), 3.25 (t, J = 5.7 Hz, 2H), 3.09 (t, J = 5.7 Hz, 2H), 2.42 (s, 3H). **^{13}C NMR** (101 MHz, $CDCl_3$) δ 186.07, 176.00, 163.66, 159.58, 159.00, 156.09, 155.01, 152.85, 140.31, 138.15, 135.48, 133.98, 132.49, 129.63, 129.41, 127.39, 126.95, 126.33, 125.66, 125.11, 124.07, 121.95, 121.00, 118.14, 113.74, 55.30, 32.94, 26.88, 21.41. **FT-IR:** ν = 2918, 2846, 1604, 1508, 1464, 1242, 1176, 1033, 823, 768, 530 cm^{-1}. **HRMS** (ESI) (m/z): $[M + H]^+$ calculated for $C_{33}H_{26}NO_4^+$: 500.1862; found: 500.1852.

*5-((E)-Benzylidene)-2-((E)-4-fluorobenzylidene)-9-phenyl-3,4,5,6,7,8-hexahydroacridin-1(2H)-one (**8a**).* Yellow solid (69 mg, 73% yield), **Mp:** 201−203 °C, R_f = 0.55 (5% ethyl acetate in petroleum ether); **^{1}H NMR** (400 MHz, $CDCl_3$) δ 8.23 (s, 1H), 7.64 (s, 1H), 7.47 (t, J = 7.2 Hz, 4H), 7.43−7.34 (m, 5H), 7.30 (t, J = 7.3 Hz, 1H), 7.17−7.04 (m, 4H), 3.17 (d, J = 6.4 Hz, 4H), 2.88 (t, J = 5.2 Hz, 2H), 2.46 (t, J = 6.1 Hz, 2H), 1.80−1.66 (m, 2H). **^{13}C NMR** (101 MHz, $CDCl_3$) δ 187.00, 163.91, 161.43, 159.85, 155.49, 151.50, 139.21, 137.60, 135.82, 135.61, 135.46, 131.90, 131.84, 131.76, 131.03, 130.80, 129.84, 128.33, 128.19, 127.28, 127.24, 127.15, 125.35, 115.70, 115.49, 32.74, 27.65, 27.63, 25.98, 22.72. **FT-IR:** ν = 3061, 2926, 2838, 1672, 1601, 1536, 1506, 1276, 1230, 1149, 836, 765, 697, 504 cm^{-1}. **HRMS** (m/z): $[M + H]^+$ calculated for $C_{33}H_{27}FNO^+$: 472.2077; found: 472.2077.

*5-((E)-Benzylidene)-2-((E)-4-(dimethylamino)-benzylidene)-9-phenyl-3,4,5,6,7,8-hexahydroacridin-1(2H)-one (**8b**).* Yellow solid (76 mg, 76% yield), **Mp:** 281−283 °C, R_f = 0.40 (10% ethyl acetate in petroleum ether); **^{1}H NMR** (400 MHz, $CDCl_3$) δ 8.20 (s, 1H), 7.65 (s, 1H), 7.51−7.43 (m, 4H), 7.38 (d, J = 7.7 Hz, 4H), 7.28 (d, J = 7.1 Hz, 1H), 7.25 (s, 1H), 7.12 (d, J = 7.1 Hz, 2H), 6.69 (d, J = 8.3 Hz, 2H), 3.19 (d, J = 6.2 Hz, 4H), 3.01 (s, 6H), 2.87 (s, 2H), 2.44 (d, 2H), 1.72 (d, 2H). **^{13}C NMR** (101 MHz, $CDCl_3$) δ 187.17, 159.80, 154.86, 151.10, 150.64, 139.47, 137.85, 137.77, 136.00, 132.10, 130.82, 130.24, 129.82, 128.19, 128.15, 127.38, 127.12, 126.98, 126.01, 123.67, 111.69, 40.14, 32.85, 27.69, 27.66, 26.23, 22.81. **FT-IR:** ν = 2957, 2923, 2848, 1656, 1569, 1518, 1357, 1151, 821, 697, 522 cm^{-1}. **HRMS** (m/z): $[M + H]^+$ calculated for $C_{33}H_{33}N_2O^+$: 497.2593; found: 497.2599.

*2-((E)-2,4-Dichlorobenzylidene)-5-((E)-4-methoxybenzylidene)-9-(4-methoxyphenyl)-3,4,5,6,7,8-hexahydroacridin-1(2H)-one (**8c**).* Yellow solid (88 mg, 75% yield), **Mp:** 232−235 °C, R_f = 0.65 (5% ethyl acetate in petroleum ether); **^{1}H NMR** (400 MHz, $CDCl_3$) δ 8.08 (s, 1H), 7.64 (s, 1H), 7.36 (d, J = 8.9 Hz, 3H), 7.18 (t, J = 2.2 Hz, 2H), 6.94 (q, J = 8.8 Hz, 4H), 6.86 (d, J = 8.7 Hz, 2H), 3.79 (s, 3H), 3.77 (s, 3H), 3.09 (t, J = 6.3 Hz, 2H), 2.91 (t, J = 5.7 Hz, 2H), 2.78 (t, J = 5.2 Hz, 2H), 2.38 (t, J = 6.0 Hz, 2H), 1.67−1.62 (m, 2H). **^{13}C NMR** (101 MHz, $CDCl_3$) δ 186.55, 160.06, 158.94, 158.67, 156.00, 151.46, 137.96, 135.74, 134.74, 134.10, 133.03, 132.27, 131.40, 131.34, 131.27, 131.00, 130.76, 130.19, 129.70, 128.44, 126.78, 125.02, 113.86, 113.71, 55.31, 55.16, 32.94, 27.80, 27.62, 26.29, 22.73. **FT-IR:** ν = 3062, 2936, 2838, 1671, 1601, 1535, 1510, 1459, 1281, 1245, 1156, 1031, 818, 550, 442 cm^{-1}. **HRMS** (m/z): $[M + H]^+$ calculated for $C_{35}H_{30}Cl_2NO_3^+$: 582.1603; found: 582.1607.

*5-((E)-2-Chlorobenzylidene)-9-(2-chlorophenyl)-2-((E)-4-methoxybenzylidene)-3,4,5,6,7,8-hexahydroacridin-1(2H)-one (**8d**).* Yellow solid (85 mg, 78% yield), **Mp:** 220−223 °C, R_f = 0.6 (5% ethyl acetate in petroleum ether); **^{1}H NMR** (400 MHz, $CDCl_3$) δ 8.26 (s, 1H), 7.68 (s, 1H), 7.53−7.48 (m, 1H), 7.45 (dd, J = 7.6, 1.5 Hz, 1H), 7.41−7.32 (m, 5H), 7.31−7.27 (m, 1H), 7.25−7.21 (m, 1H), 7.07 (dd, J = 5.9, 3.3 Hz, 1H), 6.93 (d, J = 8.8 Hz, 2H), 3.84 (s, 3H), 3.26−3.13 (m, 4H), 2.81−2.65 (m, 2H), 2.42 (t, J = 6.2 Hz, 2H), 1.81−1.72 (m, 2H). **^{13}C NMR** (101 MHz, $CDCl_3$) δ 186.93, 160.10, 160.07, 155.04, 148.43, 138.30, 137.36, 137.14, 136.09, 134.61, 133.31, 131.86, 131.81, 130.87, 129.52, 129.32, 128.67, 128.54, 128.44, 128.34, 127.65, 126.92, 126.21, 125.60, 113.99, 55.36, 32.73, 27.49, 26.97, 26.10, 22.59. **FT-IR:** ν = 2923, 2832, 1655, 1586, 1538, 1512, 1430, 1250, 1156, 1033, 831, 744,

https://doi.org/10.1021/acsomega.4c02058
ACS Omega 2024, 9, 36198−36219

533, 526 cm^{-1}. **HRMS** (m/z): $[M + H]^+$ calculated for $C_{34}H_{28}Cl_2NO_2^+$: 552.1497; found: 552.1499.

*(E)-6-(4-Fluorobenzylidene)-4-(4-methoxyphenyl)-2-(p-tolyl)-5,6,7,8-tetrahydroquinolin-5-ol (**9**).* White solid (80 mg, 89% yield), **Mp**: 280−282 °C, R_f = 0.4 (10% ethyl acetate in petroleum ether); **^{1}H NMR** (400 MHz, $CDCl_3$) δ 7.89 (d, J = 8.2 Hz, 2H), 7.57−7.48 (m, 3H), 7.27 (s, 2H), 7.24 (d, J = 7.5 Hz, 2H), 7.08−6.99 (m, 4H), 6.50 (s, 1H), 5.24 (d, J = 2.8 Hz, 1H), 3.90 (s, 3H), 3.48 (dt, J = 15.9, 6.9 Hz, 1H), 3.22−3.00 (m, 2H), 2.96−2.85 (m, 1H), 2.40 (s, 3H), 1.95 (d, J = 3.0 Hz, 1H). **^{13}C NMR** (101 MHz, $CDCl_3$) δ 159.77, 158.64, 156.46, 150.07, 139.75, 138.91, 136.59, 132.94, 130.80, 130.44, 130.37, 129.44, 128.39, 126.96, 126.68, 119.91, 115.36, 115.15, 113.98, 72.33, 55.39, 32.55, 23.41, 21.28. **FT-IR:** ν = 2955, 2922, 2854, 1596, 1506, 1440, 1229, 1177, 1032, 818, 564 cm^{-1}. **HRMS** (m/z): $[M + H]^+$ calculated for $C_{30}H_{27}FNO_2^+$: 452.2026; found: 452.2025.

*7-(4-Fluorophenyl)-1,3-bis(4-methoxyphenyl)-5,6,7,9,10,11-hexahydro-8H-chromeno[2,3-f]quinolin-8-one (**10**).* White solid (92 mg, 82% yield), **Mp**: 295−297 °C, R_f = 0.6 (10% ethyl acetate in petroleum ether); **^{1}H NMR** (400 MHz, $CDCl_3$) δ 7.96 (d, J = 8.6 Hz, 2H), 7.40 (s, 1H), 7.30 (t, 4H), 7.06−6.85 (m, J = 14.7, 6.6 Hz, 6H), 4.35 (s, 1H), 3.89 (s, 3H), 3.85 (s, 3H), 3.10−2.98 (m, 1H), 2.98−2.82 (m, 1H), 2.46−2.31 (m, 2H), 2.32−2.06 (m, 4H), 1.78 (d, J = 5.1 Hz, 2H). **^{13}C NMR** (101 MHz, $CDCl_3$) δ 197.28, 165.51, 160.55, 159.24, 158.44, 154.65, 145.05, 141.53, 140.08, 134.19, 131.48, 129.99, 129.91, 129.15, 128.17, 120.53, 120.44, 116.78, 115.25, 115.03, 114.27, 114.15, 113.53, 113.19, 55.53, 55.36, 38.91, 36.92, 32.03, 26.66, 24.44, 20.22. **FT-IR:** ν = 2940, 2918, 1712, 1604, 1508, 1241, 1173, 1041, 829, 576 cm^{-1}. **HRMS** (m/z): $[M + H]^+$ calculated for $C_{36}H_{31}FNO_4^+$: 560.2237; found: 560.2237.

*(E)-11-Benzylidene-7-(4-fluorophenyl)-15-phenyl-8,9,11,12,13,14-hexahydro-6H,7H-chromeno[3′,4′:5,6]-pyrano[2,3-a]acridin-6-one (**12**).* White solid (71 mg, 85% yield), **Mp**: 287−290 °C, R_f = 0.65 (10% ethyl acetate in petroleum ether); **^{1}H NMR** (400 MHz, $CDCl_3$) δ 8.08 (s, 1H), 7.53−7.42 (m, 4H), 7.42−7.30 (m, 8H), 7.23 (s, 1H), 7.15 (d, J = 8.3 Hz, 1H), 7.05−6.91 (m, 3H), 6.17 (d, J = 7.9 Hz, 1H), 4.54 (s, 1H), 3.20−3.05 (m, 1H), 3.05−2.95 (m, 1H), 2.90 (m, 1H), 2.86−2.76 (m, 1H), 2.47 (dt, J = 15.1, 8.1 Hz, 1H), 2.40 (t, J = 6.2 Hz, 1H), 2.38−2.23 (m, 2H), 1.79−1.62 (m, 2H). **^{13}C NMR** (101 MHz, $CDCl_3$) δ 161.47, 155.60, 155.19, 152.11, 151.36, 143.76, 142.02, 139.91, 138.33, 137.96, 135.85, 131.65, 130.21, 130.13, 129.95, 129.74, 128.85, 128.61, 128.56, 128.43, 128.10, 127.79, 127.71, 126.81, 123.49, 123.32, 120.93, 117.25, 116.12, 115.54, 115.33, 113.98, 102.94, 40.63, 32.36, 28.32, 27.79, 25.47, 23.09. **FT-IR:** ν = 2931, 2845, 1708, 1622, 1492, 1384, 1228, 1173, 757, 705, 551 cm^{-1}. **HRMS** (m/z): $[M + H]^+$ calculated for $C_{42}H_{31}FNO_3^+$: 616.2288; found: 616.2288.

■ ASSOCIATED CONTENT

Supporting Information

The Supporting Information is available free of charge at https://pubs.acs.org/doi/10.1021/acsomega.4c02058.

Copies of ^{1}H, ^{13}C NMR, mass, and IR spectra of the synthesized products, mechanism probe, 2D-NMR spectroscopic studies, photophysical properties, and X-ray crystallography data (PDF)

Crystallography data of $C_{23}H_{21}NO_2$ (CIF)

Crystallography data of $C_{31}H_{27}NO_4$ (CIF)

■ AUTHOR INFORMATION

Corresponding Author

Fazlur Rahman Nawaz Khan − *Organic and Medicinal Chemistry Research Laboratory, School of Advanced Sciences, Vellore Institute of Technology, Vellore 632014 Tamil Nadu, India;* orcid.org/0000-0001-7828-526X; Email: nawaz_f@yahoo.co.in

Author

Sundararajan Suresh − *Organic and Medicinal Chemistry Research Laboratory, School of Advanced Sciences, Vellore Institute of Technology, Vellore 632014 Tamil Nadu, India*

Complete contact information is available at: https://pubs.acs.org/10.1021/acsomega.4c02058

Author Contributions

All authors contributed to the writing of the manuscript.

Notes

The authors declare no competing financial interest.

■ ACKNOWLEDGMENTS

The authors are thankful to SIF-VIT for providing NMR, GC-MS, IR, and HRMS instrumentation facilities.

■ REFERENCES

(1) Nie, B.; Wu, W.; Zhang, Y.; Jiang, H.; Zhang, J. Recent Advances in the Synthesis of Bridgehead (or Ring-Junction) Nitrogen Heterocycles: Via Transition Metal-Catalyzed C-H Bond Activation and Functionalization. *Org. Chem. Front.* **2020**, *7*, 3067−3099.

(2) Sridharan, V.; Suryavanshi, P. A.; Menéndez, J. C. Advances in the Chemistry of Tetrahydroquinolines. *Chem. Rev.* **2011**, *111*, 7157−7259.

(3) Teja, C.; Khan, F. R. N. Radical Transformations towards the Synthesis of Quinoline: A Review. *Chem. - Asian J.* **2020**, *15*, 4153−4167.

(4) Teja, C.; Nawaz Khan, F. R. Recent Advances in the Synthesis of Thienoquinolines (Quinoline-Fused Heterocycle). *Asian J. Org. Chem.* **2020**, *9*, 1889−1900.

(5) Suman, P.; Tomar, K.; Nishad, C. S.; Banerjee, B. Metal-Free Synthesis of Carbamoylated Dihydroquinolinones via Cascade Radical Annulation of Cinnamamides with Oxamic Acids. *Org. Biomol. Chem.* **2024**, *22*, 1821−1833.

(6) Gensicka-Kowalewska, M.; Cholewiński, G.; Dzierzbicka, K. Recent Developments in the Synthesis and Biological Activity of Acridine/Acridone Analogues. *RSC Adv.* **2017**, *7*, 15776−15804.

(7) Vaz, W. F.; Custodio, J. M. F.; D'Oliveira, G. D. C.; Neves, B. J.; Junior, P. S. C.; Filho, J. T. M.; Andrade, C. H.; Perez, C. N.; Silveira-Lacerda, E. P.; Napolitano, H. B. Dihydroquinoline Derivative as a Potential Anticancer Agent: Synthesis, Crystal Structure, and Molecular Modeling Studies. *Mol. Diversity* **2021**, *25*, 55−66.

(8) Gobinath, P.; Packialakshmi, P.; Thilagavathi, G.; Elangovan, N.; Thomas, R.; Surendrakumar, R. Design, Synthesis of New 4,5-Dibenzylidene-9,10-Diphenyl-1,2,7,8,9,10 Hexahydroacridine-3,6-Dione Derivatives Using Extract of Vitexnegundo: Cytotoxic Activity & Molecular Docking Study. *Chem. Phys. Impact* **2024**, *8*, No. 100483.

(9) Kantevari, S.; Patpi, S. R.; Addla, D.; Putapatri, S. R.; Sridhar, B.; Yogeeswari, P.; Sriram, D. Facile Diversity-Oriented Synthesis and Antitubercular Evaluation of Novel Aryl and Heteroaryl Tethered Pyridines and Dihydro-6H-Quinolin-5-Ones Derived via Variants of the Bohlmann-Rahtz Reaction. *ACS Comb. Sci.* **2011**, *13*, 427−435.

(10) Shen, M.; Zhao, J.; Xu, Y.; Zhang, X.; Fan, X. Synthesis of Dihydroquinolinone Derivatives via the Cascade Reaction of O-Silylaryl Triflates with Pyrazolidinones. *J. Org. Chem.* **2021**, *86*, 15203−15216.

(11) Climent, M. J.; Corma, A.; Iborra, S.; Martí, L. Use of Mesoporous Molecular Sieves in the Production of Fine Chemicals: Preparation of Dihydroquinolinones of Pharmaceutical Interest from 2′-Aminochalcones. *ChemCatChem* **2016**, *8*, 1335−1345.
(12) Niu, Y. N.; Tian, L. S.; Lv, H. Z.; Li, P. G. Recent Advances for the Synthesis of Dihydroquinolin-2(1H)-Ones via Catalytic Annulation of α,β-Unsaturated N-Arylamides. *Catalysts* **2023**, *13*, 1105.
(13) Kim, Y. M.; Yoo, H. S.; Son, S. H.; Kim, G. Y.; Jang, H. J.; Kim, D. H.; Kim, S. D.; Park, B. Y.; Kim, N. J. A Novel Approach to N-Tf 2-Aryl-2,3-Dihydroquinolin- 4(1H)-Ones via a Ligand-Free Pd(II)-Catalyzed Oxidative Aza-Michael Cyclization. *Eur. J. Org. Chem.* **2021**, *2021*, 618−622.
(14) Sharma, D.; Kumar, M.; Kumar, S.; Basu, A.; Bhattacherjee, D.; Chaudhary, A.; Das, P. Application of Cyclohexane-1,3-Diones in the Synthesis of Six-Membered Nitrogen-Containing Heterocycles. *ChemistrySelect* **2022**, *7*, No. e202200622.
(15) Goswami, L.; Gogoi, S.; Gogoi, J.; Boruah, R. K.; Boruah, R. C.; Gogoi, P. Facile Diversity-Oriented Synthesis of Polycyclic Pyridines and Their Cytotoxicity Effects in Human Cancer Cell Lines. *ACS Comb. Sci.* **2016**, *18*, 253−261.
(16) Schuppe, A. W.; Huang, D.; Chen, Y.; Newhouse, T. R. Total Synthesis of (−)-Xylogranatopyridine B via a Palladium-Catalyzed Oxidative Stannylation of Enones. *J. Am. Chem. Soc.* **2018**, *140*, 2062−2066.
(17) Kumar, A.; Sharma, S.; Tripathi, V. D.; Maurya, R. A.; Srivastava, S. P.; Bhatia, G.; Tamrakar, A. K.; Srivastava, A. K. Design and Synthesis of 2,4-Disubstituted Polyhydroquinolines as Prospective Antihyperglycemic and Lipid Modulating Agents. *Bioorg. Med. Chem.* **2010**, *18*, 4138−4148.
(18) Ray, S.; Brown, M.; Bhaumik, A.; Dutta, A.; Mukhopadhyay, C. A New MCM-41 Supported HPF6 Catalyst for the Library Synthesis of Highly Substituted 1,4-Dihydropyridines and Oxidation to Pyridines: Report of One-Dimensional Packing towards LMSOMs and Studies on Their Photophysical Properties. *Green Chem.* **2013**, *15*, 1910−1924.
(19) Ray, S.; Banerjee, B.; Bhaumik, A.; Mukhopadhyay, C. Copper Incorporated Nanorod like Mesoporous Silica for One Pot Aerobic Oxidative Synthesis of Pyridines. *Catal. Commun.* **2015**, *58*, 97−102.
(20) Hu, X. M.; Yang, J.; Yang, J. M.; Shao, B. N.; Huang, R.; Yan, S. J. Fe(OTf)3-Catalyzed Annulation of α,β-Unsaturated Ketoxime Acetates with Enaminones for the Synthesis of Functionalized 2,4-Diarylpyridines. *Org. Chem. Front.* **2023**, *10*, 4298−4304.
(21) Vasilyev, E. S.; Agafontsev, A. M.; Tkachev, A. V. Microwave-Assisted Synthesis of Chiral Nopinane-Annelated Pyridines by Condensation of Pinocarvone Oxime with Enamines Promoted by FeCl3 and CuCl2. *Synth. Commun.* **2014**, *44*, 1817−1824.
(22) Hessel, V.; Tran, N. N.; Asrami, M. R.; Tran, Q. D.; Long, N. V. D.; Escribà-Gelonch, M.; Tejada, J. O.; Linke, S.; Sundmacher, K. Sustainability of Green Solvents-Review and Perspective. *Green Chem.* **2022**, *24*, 410−437.
(23) Khandelwal, S.; Tailor, Y. K.; Kumar, M. Deep Eutectic Solvents (DESs) as Eco-Friendly and Sustainable Solvent/Catalyst Systems in Organic Transformations. *J. Mol. Liq.* **2016**, *215*, 345−386.
(24) Veitía, M.-I.; Ferroud, C. New Activation Methods Used in Green Chemistry for the Synthesis of High Added Value Molecules. *Int. J. Energy Environ. Eng.* **2015**, *6*, 37−46.
(25) Ünlü, A. E.; Arlkaya, A.; Takaç, S. Use of Deep Eutectic Solvents as Catalyst: A Mini-Review. *Green Process. Synth.* **2019**, *8*, 355−372.
(26) Shah, P. A.; Chavda, V.; Hirpara, D.; Sharma, V. S.; Shrivastav, P. S.; Kumar, S. Exploring the Potential of Deep Eutectic Solvents in Pharmaceuticals: Challenges and Opportunities. *J. Mol. Liq.* **2023**, *390*, No. 123171.
(27) Alonso, D. A.; Baeza, A.; Chinchilla, R.; Guillena, G.; Pastor, I. M.; Ramón, D. J. Deep Eutectic Solvents: The Organic Reaction Medium of the Century. *Eur. J. Org. Chem.* **2016**, *2016*, 612−632.
(28) Abbott, A. P.; Edler, K. J.; Page, A. J. Deep Eutectic Solvents—The Vital Link between Ionic Liquids and Ionic Solutions. *J. Chem. Phys.* **2021**, *155*, No. 150401.
(29) Smith, E. L.; Abbott, A. P.; Ryder, K. S. Deep Eutectic Solvents (DESs) and Their Applications. *Chem. Rev.* **2014**, *114*, 11060−11082.
(30) Prabhune, A.; Dey, R. Green and Sustainable Solvents of the Future: Deep Eutectic Solvents. *J. Mol. Liq.* **2023**, *379*, No. 121676.
(31) Liu, P.; Hao, J. W.; Mo, L. P.; Zhang, Z. H. Recent Advances in the Application of Deep Eutectic Solvents as Sustainable Media as Well as Catalysts in Organic Reactions. *RSC Adv.* **2015**, *5*, 48675−48704.
(32) Kumar, S. L.; Servesh, A.; Sriwastav, Y. K.; Balasubramanian, S.; Tabassum, S.; Govindaraju, S. A Bird's-Eye View on Deep Eutectic Solvent-Mediated Multicomponent Synthesis of N-Heterocycles. *ChemistrySelect* **2023**, *8*, No. e202301054.
(33) Di Carmine, G.; Abbott, A. P.; D'Agostino, C. Deep Eutectic Solvents: Alternative Reaction Media for Organic Oxidation Reactions. *React. Chem. Eng.* **2021**, *6*, 582−598.
(34) Teja, C.; Nawaz Khan, F. R. Choline Chloride-Based Deep Eutectic Systems in Sequential Friedländer Reaction and Palladium-Catalyzed Sp3 CH Functionalization of Methyl Ketones. *ACS Omega* **2019**, *4*, 8046−8055.
(35) Pavithra, D.; Ethiraj, K. R.; Nawaz Khan, F. R. Cu-TEMPO Catalyzed Dehydrogenative Friedlander Annulation/Sp3 C−H Functionalization/Spiroannulation towards Spiro[Indoline-3,3′-Pyrrolizin]-2′-Yl)-4-Phenylquinoline-3-Carboxylates. *Eur. J. Org. Chem.* **2020**, *2020*, 7035−7050.
(36) Prameela, S.; Nawaz Khan, F. R. Ru-Catalyzed Sequential Dehydrogenative Friedlander Reaction/Sp3 C−H Activation/Knovenagel Condensation in the Regioselective Synthesis of Chimanine B Analogues. *Eur. J. Org. Chem.* **2020**, *2020*, 2888−2903.
(37) Prameela, S.; Nawaz Khan, F. R. Ir(I)-Catalyzed Synthesis of (E)-4-Benzylidenylacridines and (E)-2-Styrylquinoline-3-Carboxamide through Sequential Suzuki−Miyaura Coupling, Dehydrogenative Friedländer Reaction, and Sp3-C−H Activation. *Eur. J. Org. Chem.* **2020**, *2020*, 5394−5410.
(38) Teja, C.; Nawaz Khan, F. R. Tetrabutylammonium-Bromide-Promoted Synthesis of Spirooxindoles through Alkyne-Aldehyde C−C Coupling and 1,3-Dipolar Cycloaddition Using Ytterbium Triflate Catalyst. *ChemistrySelect* **2020**, *5*, 6470−6474.
(39) Nagarajan, S.; Fazlur-Rahman, N. K. Mn-Catalyzed Ligand-Free One-Pot Synthesis of (E)-6,7-Dihydrodibenzo[b,j][1,7]-Phenanthrolines and (E)-1,2,3,4-Tetrahydrobenzo[b][1,6]-Naphthyridines through Dehydrogenative Friedlander Annulation/C(Sp3)-H Functionalization. *ACS Omega* **2024**, *9*, 24464−24476.
(40) Ito, T.; Seidel, F. W.; Jin, X.; Nozaki, K. TEMPO as a Hydrogen Atom Transfer Catalyst for Aerobic Dehydrogenation of Activated Alkanes to Alkenes. *J. Org. Chem.* **2022**, *87*, 12733−12740.
(41) Soo Kim, S.; Rajagopal, G. Efficient Aerobic Oxidation of Alcohols to Carbonyl Compounds with NHPI/CAN Catalytic System. *Synth. Commun.* **2004**, *34*, 2237−2243.
(42) Pavithra, D.; Ethiraj, K. R. Tetrabutylammonium Bromide (TBAB) Promoted Metal-Free Synthesis of 2H-Indazolo[1,2-b]-Phthalazinetriones and Pyrazolo[1,2-b]Phthalazines from Benzylalcohol through Aerobic Oxidation, Sequential Addition-Cyclization with Phthalhydrazide and β-Diketones. *Polycyclic Aromat. Compd.* **2022**, *42*, 344−357.
(43) Ma, Y.; Loyns, C.; Price, P.; Chechik, V. Thermal Decay of TEMPO in Acidic Media via an N-Oxoammonium Salt Intermediate. *Org. Biomol. Chem.* **2011**, *9*, 5573−5578.
(44) Chen, Z.; Li, H.; Liao, Y.; Wang, M.; Su, W. Direct Synthesis of Alkylated 4-Hydroxycoumarin Derivatives via a Cascade Cu-Catalyzed Dehydrogenation/Conjugate Addition Sequence. *Chem. Commun.* **2023**, *59*, 6686−6689.
(45) Teja, C.; Nawaz Khan, F. R. Facile Synthesis of 2-Acylthieno[2,3- b]Quinolines via Cu-TEMPO-Catalyzed Dehydrogenation, Sp2-C−H Functionalization (Nucleophilic Thiolation by S8) of 2-Haloquinolinyl Ketones. *Org. Lett.* **2020**, *22*, 1726−1730.
(46) Jie, X.; Shang, Y.; Zhang, X.; Su, W. Cu-Catalyzed Sequential Dehydrogenation-Conjugate Addition for β-Functionalization of Saturated Ketones: Scope and Mechanism. *J. Am. Chem. Soc.* **2016**, *138*, 5623−5633.

https://doi.org/10.1021/acsomega.4c02058
ACS Omega 2024, 9, 36198−36219

(47) Shang, Y.; Jie, X.; Jonnada, K.; Zafar, S. N.; Su, W. Dehydrogenative Desaturation-Relay via Formation of Multicenter-Stabilized Radical Intermediates. *Nat. Commun.* **2017**, *8* (1), No. 2273.
(48) Mohamed, M. F. A.; Abuo-Rahma, G. E. D. A. Molecular Targets and Anticancer Activity of Quinoline-Chalcone Hybrids: Literature Review. *RSC Adv.* **2020**, *10*, 31139−31155.
(49) Mezgebe, K.; Melaku, Y.; Mulugeta, E. Synthesis and Pharmacological Activities of Chalcone and Its Derivatives Bearing N-Heterocyclic Scaffolds: A Review. *ACS Omega* **2023**, *8*, 19194−19211.
(50) Jagadale, S. M.; Abhale, Y. K.; Pawar, H. R.; Shinde, A.; Bobade, V. D.; Chavan, A. P.; Sarkar, D.; Mhaske, P. C. Synthesis of New Thiazole and Pyrazole Clubbed 1,2,3-Triazol Derivatives as Potential Antimycobacterial and Antibacterial Agents. *Polycyclic Aromat. Compd.* **2022**, *42*, 3216−3237.
(51) Reddy, T. S.; Kulhari, H.; Reddy, V. G.; Bansal, V.; Kamal, A.; Shukla, R. Design, Synthesis and Biological Evaluation of 1,3-Diphenyl-1H-Pyrazole Derivatives Containing Benzimidazole Skeleton as Potential Anticancer and Apoptosis Inducing Agents. *Eur. J. Med. Chem.* **2015**, *101*, 790−805.
(52) Helguera, A. M.; Pérez-Garrido, A.; Gaspar, A.; Reis, J.; Cagide, F.; Vina, D.; Cordeiro, M. N. D. S.; Borges, F. Combining QSAR Classification Models for Predictive Modeling of Human Monoamine Oxidase Inhibitors. *Eur. J. Med. Chem.* **2013**, *59*, 75−90.
(53) Shibuguchi, T.; Mihara, H.; Kuramochi, A.; Ohshima, T.; Shibasaki, M. Catalytic Asymmetric Phase-Transfer Michael Reaction and Mannich-Type Reaction of Glycine Schiff Bases with Tartrate-Derived Diammonium Salts. *Chem. - Asian J.* **2007**, *2*, 794−801.
(54) Teja, C.; Garg, A.; Rohith, G. K.; Roshini, H.; Jena, S.; Nawaz Khan, F. R. Diversity Oriented Synthesis of Oxygen-Heterocycles, Warfarin Analogs Utilizing Microwave-Assisted Dimethyl Urea-Based Deep Eutectic Solvents. *Polycyclic Aromat. Compd.* **2022**, *42*, 4769−4779.

https://doi.org/10.1021/acsomega.4c02058
ACS Omega 2024, 9, 36198−36219